2 The adiabatic limit and beyond

The models of the form (1.1) possess a limit which simplifies the analysis a lot, the so called *adiabatic limit*, in which $\mathcal{H}$ becomes diagonal in the phonon part of the interaction. Section 2.1 will introduce this limit and discuss its relation to the full class of models. It turns out that upper and lower bounds to the free energy of the full model can be set in terms of its adiabatic limit. The interval between these bounds tells something about the use of this limit as an approximation. Having established a range of validity this way in section 2.2, the adiabatic limit is investigated in more detail. It turns out that certain correlations can be shown *not* to be present in the limit, and hence not in the range of valid approximation. This is the topic of section 2.3. The special cases of one and two sites, and of half–filling can and will be treated analytically in section 2.4.3. Section 2.5 is then devoted to the numerical simulation of the ensemble of the adiabatic model. Several static and dynamic correlations will be introduced here which will be used in chapter 5 when we map out the phase diagram of the adiabatic Holstein Model.

2.1 The adiabatic ensembles

Consider a model which satisfies property A (1.34), and hence can be transformed to

$$\mathcal{H} = \hbar a^\dagger \bullet \Omega \bullet a \; + \; :c^\dagger \cdot T \cdot c: + x \bullet :c^\dagger \cdot \Lambda \cdot c:. \tag{2.1}$$

It was mentioned in 1.1.2 that for infinitely heavy phonons, the phonon part of this transformed model reduces to

$$\mathcal{H}_{\mathsf{ph}} = \tfrac{1}{2} x \bullet K \bullet x. \tag{2.2}$$

Depending on whether before the transformation the model was of the Fröhlich or the Holstein type, this means the anti–adiabatic ($\omega \to \infty$) resp. the adiabatic limit ($\omega \to 0$). Because now $\mathcal{H}$ and x commute, analysis is greatly simplified. This section considers the thermodynamics in this limit, as much of the later derivations in this work will refer to it.

We define

$$\mathcal{H}_{\mathsf{ad}} \stackrel{\mathrm{def}}{=} \tfrac{1}{2} x \bullet K \bullet x + \; :c^\dagger \cdot Q(x) \cdot c: \tag{2.3}$$

$$Q(x) \stackrel{\mathrm{def}}{=} T + x \bullet \Lambda, \tag{2.4}$$

and

$$Z_{\mathsf{ad}} \stackrel{\mathrm{def}}{=} \mathrm{Tr} \; \exp\left[-\beta \mathcal{H}_{\mathsf{ad}}\right] = \int d\{x\} \, \exp\left[-\tfrac{1}{2}\beta x \bullet K \bullet x\right] Z_f(x), \tag{2.5}$$

$$Z_f(x) \stackrel{\mathrm{def}}{=} \mathrm{Tr}_f \; \exp\left[-\beta :c^\dagger \cdot Q(x) \cdot c:\right]. \tag{2.6}$$

In this section, Tr_f means the partial trace over all fermion states, which has a different meaning depending on whether we consider the Canonical or the Grand Canonical Ensemble. In both cases this partial trace can be performed analytically.

2.1.1 The grand canonical ensemble

In the Grand Canonical Ensemble (GCE), where the total number of particles may fluctuate, "the sum over all states" means

$$\mathrm{Tr_f}\ \ O \stackrel{\mathrm{def}}{=} \sum_{\{n_i'\}} \langle\{n_i'\}|O|\{n_i'\}\rangle, \tag{2.7}$$

in any complete eigenbasis of local number operators n_i, for any operator O. The bra and ket are defined by

$$|\{n_i'\}\rangle \stackrel{\mathrm{def}}{=} c_1^{\dagger\, n_1'} \ldots c_L^{\dagger\, n_L'} |\mathrm{vac}\rangle. \tag{2.8}$$

For any matrix A that commutes with the fermion creation and annihilation operators,

$$\sum_{\{n'\}} \langle\{n_i'\}|\exp\left[:c^\dagger \cdot A \cdot c:\right]|\{n'\}\rangle = \det\left(2\cosh\tfrac{1}{2}A\right). \tag{2.9}$$

This is easily proven by diagonalization of $A = S^\dagger \cdot \alpha \cdot S$, as

$$\begin{aligned}
\mathrm{Tr_f}\exp\left[:c^\dagger \cdot A \cdot c:\right] &= \sum_{\{n'\}} \langle\{n'\}|\exp\left[:c^\dagger \cdot S^\dagger \cdot \alpha \cdot S \cdot c:\right]|\{n'\}\rangle \\
&= \sum_{\{n'\}} \langle\{n'\}|\exp\left[\sum_i \alpha_i (n_i - \tfrac{1}{2})\right]|\{n'\}\rangle \\
&= \prod_i \sum_{n_i'=0,1} \langle n_i'|e^{\alpha_i (n_i - \frac{1}{2})}|n_i'\rangle \\
&= \prod_i \left(e^{-\frac{1}{2}\alpha_i} + e^{+\frac{1}{2}\alpha_i}\right) \\
&= \prod_i 2\cosh\tfrac{1}{2}\alpha_i \\
&= \det\left(2\cosh\tfrac{1}{2}A\right),
\end{aligned} \tag{2.10}$$

where $n_i = (c^\dagger \cdot S^\dagger)_i (S \cdot c\ )_i$, the number operators in the new basis, and n_i' their eigenvalues. Using (2.9), (2.6) can be evaluated as

$$Z_f(x) \stackrel{\mathrm{def}}{=} \mathrm{Tr_f}\ \ \exp\left[-\beta\, :c^\dagger \cdot Q(x) \cdot c:\right] = \det\left(2\cosh\tfrac{1}{2}\beta Q(x)\right). \tag{2.11}$$

Note that the chemical potential μ is implicit in Q. We now define an effective Hamiltonian

$$\mathcal{H}_{\mathrm{eff}} \stackrel{\mathrm{def}}{=} \tfrac{1}{2} x \bullet K \bullet x - \beta^{-1} \log Z_f(x) \tag{2.12}$$

then

$$Z_{\mathrm{ad}} = \int d\{x\} \exp\left[-\beta \mathcal{H}_{\mathrm{eff}}(x)\right] \tag{2.13}$$

describes the thermodynamics of a classical problem, albeit with a complicated (and temperature dependent) interaction between the coordinates x_i. Expectation values of the adiabatic ensemble can now be decomposed as

$$\langle\, O \,\rangle_{ad} = \langle\langle\, \overline{O} \,\rangle\rangle, \tag{2.14}$$

$$\langle\langle\, O \,\rangle\rangle \stackrel{\text{def}}{=} Z_{ad}^{-1} \int d\{x\} \exp\left[-\beta \mathcal{H}_{\text{eff}}(x)\right] O, \tag{2.15}$$

$$\overline{O} \stackrel{\text{def}}{=} Z_f^{-1}\, \mathrm{Tr}_f\ \exp\left[-\beta : c^\dagger \cdot Q(x) \cdot c :\right]. \tag{2.16}$$

Note that the inner average, over the fermion states, depends on the phonon state x. For operators O that do not contain any fermion operators, $\langle\, O \,\rangle = \langle\langle\, O \,\rangle\rangle$, but for the general case it is also necessary to express the fermion correlations in terms of Q. We define

$$W_{ij}(x) \stackrel{\text{def}}{=} \overline{c_j^\dagger c_i}. \tag{2.17}$$

Differentiating the log of (2.9) with respect to a matrix element A_{ij} gives

$$\frac{\mathrm{Tr}_f \exp\left[: c^\dagger \cdot A \cdot c : \right] c_j^\dagger c_i}{\mathrm{Tr}_f \exp\left[: c^\dagger \cdot A \cdot c : \right]} = \left(\mathbb{1} + e^{-A}\right)^{-1}_{ji}. \tag{2.18}$$

So it follows that

$$W_{ij}(x) = \left(\mathbb{1} + e^{\beta\, Q(x)}\right)^{-1}_{ji}. \tag{2.19}$$

An alternate proof of this equality that allows generalisation to higher order correlations reads

$$\begin{aligned} W_{ij} &= Z_f^{-1}\, \mathrm{Tr}_f\, e^{-\beta\ : c^\dagger \cdot Q \cdot c :} c_j^\dagger c_i \\ &= \delta_{ij} - Z_f^{-1}\, \mathrm{Tr}_f\, e^{-\beta\ : c^\dagger \cdot Q \cdot c :} c_i c_j^\dagger \\ &= \delta_{ij} - W'_{ij}, \end{aligned} \tag{2.20}$$

introducing the matrix W' for the moment. On the other hand, using cyclic invariance of the trace

$$\mathrm{Tr}\, ABC = \mathrm{Tr}\, BCA = \mathrm{Tr}\, CAB \tag{2.21}$$

and (1.33),

$$\begin{aligned} W_{ij} &= Z_f^{-1}\, \mathrm{Tr}_f\, e^{-\beta\ : c^\dagger \cdot Q \cdot c :} c_j^\dagger e^{\beta\ : c^\dagger \cdot Q \cdot c :} e^{-\beta\ : c^\dagger \cdot Q \cdot c :} c_i \\ &= Z_f^{-1}\, \mathrm{Tr}_f \sum_{j'} c_{j'}^\dagger \left(e^{-\beta Q}\right)_{j'j} e^{-\beta\ : c^\dagger \cdot Q \cdot c :} c_i \\ &= \sum_{j'} Z_f^{-1}\, \mathrm{Tr}_f\, e^{-\beta\ : c^\dagger \cdot Q \cdot c :} c_i c_{j'}^\dagger \left(e^{-\beta Q}\right)_{j'j} \\ &= \sum_{j'} W'_{ij'} \left(e^{-\beta Q}\right)_{j'j}. \end{aligned} \tag{2.22}$$

Combining these two expressions, we arrive at the matrix equations

$$W = \mathbb{1} - W' = W' \cdot e^{-\beta Q}, \tag{2.23}$$

from which it is clear that

$$W' = \left(\mathbb{1} + e^{-\beta Q}\right)^{-1}, \qquad W = \left(\mathbb{1} + e^{+\beta Q}\right)^{-1}. \tag{2.24}$$

As an example consider

$$\left\langle c^\dagger \cdot A \cdot c \right\rangle = \left\langle\!\!\left\langle \sum_{ij} A_{ij} \overline{c_i^\dagger c_j} \right\rangle\!\!\right\rangle = \left\langle\!\!\left\langle \sum_{ij} A_{ij} W_{ji} \right\rangle\!\!\right\rangle = \langle\!\langle \operatorname{Sp} AW \rangle\!\rangle. \tag{2.25}$$

The technique of the above proof applied to higher order fermion correlations yields

$$\overline{c_{i_1}^\dagger \ldots c_{i_n}^\dagger c_{j_1} \ldots c_{j_n}} = \sum_{i'} \overline{c_{i_2}^\dagger \ldots c_{i_n}^\dagger c_{j_1} \ldots c_{j_n} c_{i'}^\dagger} \left(e^{-\beta Q}\right)_{i' i_1}, \tag{2.26}$$

and (anti)commuting $c_{i_1}^\dagger$ all the way through the right gives

$$\overline{c_{i_1}^\dagger \ldots c_{i_n}^\dagger c_{j_1} \ldots c_{j_n}} = - \overline{c_{i_2}^\dagger \ldots c_{i_n}^\dagger c_{j_1} \ldots c_{j_n} c_{i_1}^\dagger} + \sum_{l=1}^{n} (-)^l \overline{c_{i_2}^\dagger \ldots c_{i_n}^\dagger c_{j_1} \ldots \delta_{i_1 j_l} \ldots c_{j_n}}. \tag{2.27}$$

Combining these two we get after some manipulations

$$\sum_{i'} \overline{c_{i_2}^\dagger \ldots c_{i_n}^\dagger c_{j_1} \ldots c_{j_n} c_{i'}^\dagger} \left(\mathbb{1} + e^{-\beta Q}\right)_{i' i_1} = \sum_{l=1}^{n} (-)^l \delta_{i_1 j_l} \overline{c_{i_2}^\dagger \ldots c_{i_n}^\dagger c_{j_1} \ldots \not{c}_{j_l} \ldots c_{j_n}}, \tag{2.28}$$

ie. the annihilator with index j_l is crossed out. With the aid of (2.26) and (2.17) the above can be rewritten as

$$\overline{c_{i_1}^\dagger \ldots c_{i_n}^\dagger c_{j_1} \ldots c_{j_n}} = \sum_{l=1}^{n} (-)^l W_{i_1 j_l} \overline{c_{i_2}^\dagger \ldots c_{i_n}^\dagger c_{j_1} \ldots \not{c}_{j_l} \ldots c_{j_n}}, \tag{2.29}$$

from which relations like eg.

$$\overline{c_i^\dagger c_j^\dagger c_k c_l} = W_{il} W_{jk} - W_{ik} W_{jl} \tag{2.30}$$

can be derived.

Thus we have a recursion relation to express an n–point correlation as a sum of $(n-2)$–point correlations. This is nothing but Wick's theorem[7] in disguise. Note that all correlations with unequal numbers of creation and annihilation operators must vanish. Hence, if the two–point correlations (2.17) are known, this allows all n-point fermion correlations to be expressed as closed forms in x, averaged with (2.15). Evaluation of these averages over x_i is accessible to standard numerical techniques. Section 2.5 will be devoted to this.

2.1.2 The canonical ensemble

In the Canonical Ensemble (CE) the total number of particles N is fixed. The chemical potential implicit in T and Q can be set to zero, and the trace of an operator O is defined by

$$\mathrm{Tr_f}\ \mathrm{O} \stackrel{\mathrm{def}}{=} \sum_{i_1 \ldots i_N} \langle i_1 \ldots i_N | \mathrm{O} | i_1 \ldots i_N \rangle, \tag{2.31}$$

where

$$|i_1 \ldots i_N\rangle \stackrel{\mathrm{def}}{=} c^\dagger_{i_1} \ldots c^\dagger_{i_N} |\mathrm{vac}\rangle. \tag{2.32}$$

These spaces are orthogonal for different N. Together they span the space used in the grand canonical ensemble. On each of these subspaces, (2.31) defines a proper trace.

The different form of the trace has as a consequence that (2.10) must be replaced by

$$\begin{aligned} \mathrm{Tr_f} \exp :c^\dagger \cdot A \cdot c: &= e^{-\mathrm{Sp}\, A/2} \sum_{i_1 \ldots i_N} \langle i_1 \ldots i_N | \exp c^\dagger \cdot A \cdot c | i_1 \ldots i_N \rangle \\ &= e^{-\mathrm{Sp}\, A/2} \sum_{i_1 \ldots i_N} \sum_{j_1 \ldots j_N} \langle i_1 \ldots i_N | j_1 \ldots j_N \rangle \left(e^A\right)_{i_1 j_1} \ldots \left(e^A\right)_{i_N j_N} \\ &= e^{-\mathrm{Sp}\, A/2} \sum_{i_1 \ldots i_N} \begin{vmatrix} \left(e^A\right)_{i_1 i_1} & \ldots & \left(e^A\right)_{i_1 i_N} \\ \vdots & \ddots & \vdots \\ \left(e^A\right)_{i_N i_1} & \ldots & \left(e^A\right)_{i_N i_N} \end{vmatrix}. \end{aligned} \tag{2.33}$$

The second step follows by substituting (2.32) for the basis ket, inserting the identity operator $\mathbb{1} = \exp\left[-c^\dagger \cdot A \cdot c\right] \exp\left[c^\dagger \cdot A \cdot c\right]$ between the creation operators and using (1.33). Now the N–particle partial partition sum becomes

$$\begin{aligned} Z_f(x) &\stackrel{\mathrm{def}}{=} \mathrm{Tr_f}\ \exp\left[-\beta :c^\dagger \cdot Q(x) \cdot c:\right] \\ &= e^{\beta\, \mathrm{Sp}\, Q/2} \sum_{i_1 \ldots i_N} \begin{vmatrix} \left(e^{-\beta Q}\right)_{i_1 i_1} & \ldots & \left(e^{-\beta Q}\right)_{i_1 i_N} \\ \vdots & \ddots & \vdots \\ \left(e^{-\beta Q}\right)_{i_N i_1} & \ldots & \left(e^{-\beta Q}\right)_{i_N i_N} \end{vmatrix}. \end{aligned} \tag{2.34}$$

As a limiting case, for a single particle, $N = 1$,

$$\mathrm{Tr_f}\ \exp\left[-\beta :c^\dagger \cdot Q(x) \cdot c:\right] = e^{\beta\, \mathrm{Sp}\, Q/2} \sum_i \left(\exp\left[-\beta Q(x)\right]\right)_{ii} = e^{\beta\, \mathrm{Sp}\, Q/2}\, \mathrm{Sp}\, e^{-\beta Q}. \tag{2.35}$$

After replacing (2.11) by (2.34) the definition of $\mathcal{H}_{\mathrm{eff}}$, equation (2.12) and the decomposition of the expectation value (2.14) can be used without modification.

Now the expression for W can be evaluated much like Z_f was. Introduce again

$$W'_{ij} = \delta_{ij} - W_{ij} = \overline{c_l c^\dagger_k}, \tag{2.36}$$

then use

$$\begin{aligned} &\langle i_1 \ldots i_N | \exp\left[-\beta :c^\dagger \cdot Q \cdot c:\right] c_l c^\dagger_k | i_1 \ldots i_N \rangle \\ &\qquad = \sum_{l'} \langle i_1 \ldots i_N l' | \exp\left[-\beta :c^\dagger \cdot Q \cdot c:\right] | i_1 \ldots i_N k \rangle \left(e^{-\beta Q}\right)_{ll'}, \end{aligned} \tag{2.37}$$

to arrive at

$$\overline{c_l c_k^\dagger} = Z_f^{-1} \exp \beta \operatorname{Sp} Q/2 \sum_{i_1 \ldots i_N} \begin{vmatrix} \delta_{kl} & \left(e^{-\beta Q}\right)_{i_1 l} & \cdots & \left(e^{-\beta Q}\right)_{i_N l} \\ \delta_{k i_1} & \left(e^{-\beta Q}\right)_{i_1 i_1} & \cdots & \left(e^{-\beta Q}\right)_{i_N i_1} \\ \vdots & \vdots & \ddots & \vdots \\ \delta_{k i_N} & \left(e^{-\beta Q}\right)_{i_1 i N} & \cdots & \left(e^{-\beta Q}\right)_{i_N i_N} \end{vmatrix} . \qquad (2.38)$$

Higher order correlations follow in similar ways. Eg. for $N = 1$,

$$W_{ij}^\dagger = Z_f^{-1} \left(e^{-\beta Q(x)}\right)_{ij} . \qquad (2.39)$$

With these results for Z_f and W in the canonical ensemble a small paradox arises. It would seem that the derivation of (2.24) for the grand canonical ensemble could be carried over to the canonical ensemble without modification, as the only ingredients we used were (1.33), and cyclic invariance of the trace (2.21) in going from the second to the third line in (2.22). Of course, cyclic invariance is a property of *any* proper trace. The tricky part lies in the fact that (2.21) does not hold when any of the operators does not leave the subspace on which the trace works invariant, in the case at hand, for any operator that does not preserve the number of particles, like $c^\dagger$ and c . Thus (2.22) breaks down, and there is no contradiction with (2.34) and (2.38).

2.1.3 Relation to quenched disorder models

The decomposition of the thermodynamical average into a phonon and an electron part bears a similarity to a simple model for "quenched disorder", ie. random fluctuations that are not of thermal nature (and hence not governed by a temperature), but are frozen in like, say, impurities in experimental samples. A simple model for these is given by a tight binding model of the form $c^\dagger \cdot Q(x) \cdot c$ where the x are not the phonon coordinates but disorder coordinates coupled to the local potential felt by electrons, and typically drawn from a Gaussian distribution. Apart from the thermodynamical average $\overline{O}$ per sample, one "ensemble–averages" $\langle\langle \overline{O} \rangle\rangle$ over disorder realisations. With $\langle\langle O \rangle\rangle$ like before, but replacing $\mathcal{H}_{\text{eff}}$ with a simple quadratic form this is summarized as

$$\langle\langle \overline{O} \rangle\rangle = Z^{-1} \int d\{x\} \exp\left[-\tfrac{1}{2}\gamma x \bullet x\right] \overline{O}. \qquad (2.40)$$

We note that for parameter values for which the $\log Z_f$ term in $\mathcal{H}_{\text{eff}}$ is nearly constant as a function of x (eg. weak coupling), and with the role of the disorder strength γ taken by βK, we may expect that the effect of the phonons is like that of quenched disorder. Apart from this qualitative hint about the physics of the system in terms of this disorder, the analogy is even more fruitful when applied in the other direction: from the computer program to simulate the electron–phonon model (introduced in section 2.5) one only has to remove the lines adding $-\beta^{-1} \log Z_f$ to the Hamiltonian to obtain a perfect simulation of these quenched disorder models.

2.2 Bounds to the free energy

Having introduced the adiabatic limit, it is appropriate to try to estimate a range of validity of its use as an approximation to non–limiting cases. This shall be the purpose of the current

section [1].

Trotter–Suzuki decompositions of the free energy (1.37) can be used to set lower bounds to it, using the Golden–Symanzik–Thompson inequality

$$\operatorname{Tr} e^{A+B} \leq \operatorname{Tr} e^{A} e^{B} \tag{2.41}$$

and Jensen's Inequality[5]

$$\operatorname{Tr} e^{A+B} = \operatorname{Tr} e^{A} e^{-A} e^{A+B} \geq \exp\left\{ \frac{\operatorname{Tr} e^{A} B}{\operatorname{Tr} e^{A}} \right\} \operatorname{Tr} e^{A}, \tag{2.42}$$

which both hold for sufficiently nice A and B. From these inequalities one derives that for any two Hamiltonians $\mathcal{H}_1$ and $\mathcal{H}_2$, if $\mathcal{H}_{1+2} = \mathcal{H}_1 + \mathcal{H}_2$ etc., the following upper and lower bounds to F_{1+2} hold:

$$-\beta^{-1} \log \operatorname{Tr} e^{-\beta \mathcal{H}_1} e^{-\beta \mathcal{H}_2} \leq F_{1+2} \leq \langle \mathcal{H}_2 \rangle_1 + F_1. \tag{2.43}$$

Although the quality of these bounds of F says *nothing* about its derivatives, the correlation functions, and their corresponding approximations, a bad bound is a good indication of a bad approximation.

2.2.1 A lower bound

A useful family of lower bounds to the free energy of the full model is obtained by splitting (1.1) into a pure phonon part and a part diagonal in x. Consider the decomposition parametrized by $\gamma \in [0,1]$

$$\begin{aligned} Z_1(\gamma) &= \operatorname{Tr} \exp\left[-\tfrac{1}{2}\beta\,(p \bullet p + \gamma x \bullet K \bullet x)\right] \exp\left[-\tfrac{1}{2}\beta\left((1-\gamma) x \bullet K \bullet x + 2 : c^{\dagger} \cdot Q(x) \cdot c :\right)\right] \\ &= \int d\{x'\} \langle \{x'\} | \exp\left[-\tfrac{1}{2}\beta\,(p \bullet p + \gamma x \bullet K \bullet x)\right] | \{x'\} \rangle \times \\ &\qquad \times \operatorname{Tr}_f \exp\left[-\tfrac{1}{2}\beta\left((1-\gamma) x' \bullet K \bullet x' + 2 : c^{\dagger} \cdot Q(x') \cdot c :\right)\right]. \end{aligned} \tag{2.44}$$

Here, $Q = T + x \bullet \Lambda$ as before, and as K is taken to be diagonal, $K_{ij} = \delta_{ij} M \omega_i^2$, the first factor can be worked out with the textbook[6] expression

$$\begin{aligned} &\langle x | \exp\left\{ -\beta \left[\frac{p^2}{2M} + \tfrac{1}{2} M \omega^2 x^2 \right] \right\} | y \rangle = \\ &\qquad \left(\frac{M\omega}{2\pi\hbar \sinh \beta\hbar\omega} \right)^{\frac{1}{2}} \exp\left\{ \frac{M\omega}{2\hbar \sinh \beta\hbar\omega} \left[(x^2 + y^2) \cosh \beta\hbar\omega - 2xy \right] \right\}, \end{aligned} \tag{2.45}$$

where we have to substitute $\omega \to \sqrt{\gamma}\omega$. In the second factor of (2.44) we recognize the effective Hamiltonian of (2.12) but for the rescaling of K by the factor $(1-\gamma)$. Substituting these results in

$$Z_1(\gamma) = \prod_i \left(\frac{\sqrt{\gamma}\omega_i}{2\pi\hbar \sinh \beta\hbar\sqrt{\gamma}\omega_i} \right)^{\frac{1}{2}} \int d\{x'\} \exp\left[-\beta \tilde{\mathcal{H}}_{\text{eff}}(x') \right] \tag{2.46}$$

[1] This section is based on the publication[31].

where

$$\tilde{\mathcal{H}}_{\text{eff}}(x) = \tfrac{1}{2} x \bullet \tilde{K} \bullet x - \beta^{-1} \log Z_f(x) \tag{2.47}$$

$$\tilde{K}(\gamma)_{ij} = \delta_{ij} M \omega_i^2 [(1-\gamma) + \gamma \eta(\beta \hbar \sqrt{\gamma} \omega_i / 2)] \tag{2.48}$$

$$\eta(\alpha) = \frac{\tanh \alpha}{\alpha} = \frac{\cosh 2\alpha - 1}{\alpha \sinh 2\alpha}. \tag{2.49}$$

In the first factor of (2.46) we now recognize the free phonon partition function, the second part is equal to the partition function of the adiabatic model with spring constants $\tilde{K}(\gamma)$. Application of (2.41) gives

$$F_{\text{ad}}(K) \leq F_{\text{ph}}(\sqrt{\gamma}\omega) + F_{\text{ad}}(\tilde{K}(\gamma)) \leq F. \tag{2.50}$$

The first of these inequalities follows from the fact that the bound assumes a minimum for $\gamma = 0$. The second bound may be maximized for $\gamma \in [0, 1]$.

2.2.2 An upper bound

An upper bound to F in terms of F_{ad} can be derived by writing $x = \bar{x} + x_0$, with x_0 some constant and

$$\begin{aligned} \mathcal{H}_0 &= \tfrac{1}{2} p \bullet p + \tfrac{1}{2} \bar{x} \bullet K \bullet \bar{x} + \tfrac{1}{2} x_0 \bullet K \bullet x_0 + x_0 \bullet : c^\dagger \cdot \Lambda \cdot c : + : c^\dagger \cdot T \cdot c : \\ \mathcal{H} - \mathcal{H}_0 &= \tfrac{1}{2} \bar{x} \bullet K \bullet x_0 + \tfrac{1}{2} x_0 \bullet K \bullet \bar{x} + \bar{x} \bullet : c^\dagger \cdot \Lambda \cdot c : . \end{aligned} \tag{2.51}$$

Define

$$\begin{aligned} Z_0(x_0) &= \operatorname{Tr} \exp\left[-\tfrac{1}{2}\beta \left[p \bullet p + \bar{x} \bullet K \bullet \bar{x}\right]\right] \exp\left[-\beta \tfrac{1}{2} x_0 \bullet K \bullet x_0\right] \exp\left[-\beta : c^\dagger \cdot Q(x_0) \cdot c :\right] \\ &= Z_{\text{ph}} \exp\left[-\beta \mathcal{H}_{\text{eff}}(x_0)\right], \end{aligned} \tag{2.52}$$

where Z_{ph} is again the partition function of the free phonons, and let $\langle \ldots \rangle_0$ denote the corresponding thermodynamic average over fermionic degrees of freedom and the $\bar{x}$, then taking the log of Z_0, we can use (2.42) to write

$$F \leq F_{\text{ph}}(\omega) + \mathcal{H}_{\text{eff}}(x_0) + \langle \mathcal{H} - \mathcal{H}_0 \rangle_0. \tag{2.53}$$

Note that

$$\langle \mathcal{H} - \mathcal{H}_0 \rangle_0 = 0 \tag{2.54}$$

by parity in $\bar{x}$. Equation (2.53) will hold for any x_0, so in particular, the free energy is bound by

$$F \leq F_{\text{ph}}(\omega) + \min_{x_0} \mathcal{H}_{\text{eff}}(x_0). \tag{2.55}$$

At zero temperature, the second term is nothing but the ground state energy of the adiabatic Hamiltonian.

2.2.3 Bounds to the ground state energy

At zero temperature, the free energy equals the ground state energy. Furthermore, (2.48) reduces to

$$\tilde{K}(\gamma) = (1-\gamma)K. \tag{2.56}$$

Combining (2.50) and (2.55) we get for the ground state energy E of the full model,

$$E_{ad} \leq \max_{\gamma\in[0,1]} \left[E_{ph}(\sqrt{\gamma}\omega) + E_{ad}([1-\gamma]K)\right] \leq E \leq E_{ph}(\omega) + E_{ad}(K). \tag{2.57}$$

All E's refer to the ground state energies of the systems that their subscripts indicate. From (2.57) it follows immediately that for low energy phonons, ie. small ω or equivalently, for large M, the upper and lower limits coalesce.

All derived bounds have been expressed either in closed form, or in terms of the energy of the adiabatic model, which will be investigated numerically in later sections. Results concerning the bounds (2.50), (2.55) and (2.57) will be presented in the context of sections 4.4 and 5.1.

2.3 Correlations and susceptibilities

To study the presence of order and disorder in a certain thermodynamic state, the proper objects of scrutiny are *correlations* and *susceptibilities*. To be specific, correlations S and susceptibilities χ, of two operators $\hat{A}, \hat{B}$, are defined by

$$S_{\hat{A}\hat{B}} = \langle\, \hat{A}^\dagger \hat{B} \,\rangle \tag{2.58}$$

$$\chi_{\hat{A}\hat{B}} = \int_0^\beta d\tau \langle\, \hat{A}^\dagger e^{-\tau\mathcal{H}} \hat{B} e^{\tau\mathcal{H}} \,\rangle. \tag{2.59}$$

One derives the inequality

$$\chi_{\hat{A}\hat{B}} \leq \frac{\beta}{2}\left(S_{\hat{A}\hat{B}} + S_{\hat{B}^\dagger\hat{A}^\dagger}\right), \tag{2.60}$$

with equality holding when either $\hat{A}$ or $\hat{B}$ commutes with $\mathcal{H}$. Susceptibilities arise when one considers the linear response of a system to a perturbation [30], eg. (2.59) follows from the definition

$$\chi_{\hat{A}\hat{B}} \stackrel{\text{def}}{=} \left.\frac{\partial}{\partial\lambda}\right|_{\lambda=0} \langle\, \hat{A} \,\rangle_{\mathcal{H}+\lambda\hat{B}}. \tag{2.61}$$

Using the expression (2.25) expectation values of quadratic forms $c^\dagger \cdot A \cdot c$ in the adiabatic ensemble were already conveniently expressed as

$$\langle\, c^\dagger \cdot A \cdot c \,\rangle = \langle\!\langle\, \mathrm{Sp}\, A \cdot W \,\rangle\!\rangle. \tag{2.62}$$

This holds for any A which commutes with x. More information can be obtained by studying correlations between higher order expressions in the fermion operators.

This section will introduce two special classes of fourth order correlations, along with some analytical results.

2.3.1 Correlations of quadratic forms

When $\hat{A}$ and $\hat{B}$ are both quadratic forms in the fermions and commute with x, expressions similar to (2.62) are obtained with the aid of the anticommutation relations and (2.30):

$$S_{\hat{A},\hat{B}} = \langle\, c^\dagger \cdot A^\dagger \cdot c\; c^\dagger \cdot B \cdot c \,\rangle = \langle\!\langle\, \mathrm{Sp}\, A^\dagger \cdot (\mathbb{1} - W) \cdot B \cdot W \,\rangle\!\rangle + \langle\!\langle\, \mathrm{Sp}\, A^\dagger \cdot W\, \mathrm{Sp}\, B \cdot W \,\rangle\!\rangle. \tag{2.63}$$

Under the same conditions one derives for the susceptibility

$$\begin{aligned}\chi_{\hat{A},\hat{B}} &= \int_0^\beta d\tau \langle\, c^\dagger \cdot A^\dagger \cdot c\, e^{-\tau\mathcal{H}} c^\dagger \cdot B \cdot c\, e^{\tau\mathcal{H}} \,\rangle \\ &= \int_0^\beta d\tau \langle\!\langle\, \mathrm{Sp}\, A^\dagger \cdot (\mathbb{1} - W) \cdot e^{-\tau Q} \cdot B \cdot e^{\tau Q} \cdot W \,\rangle\!\rangle + \beta \langle\!\langle\, \mathrm{Sp}\, A^\dagger \cdot W\, \mathrm{Sp}\, B \cdot W \,\rangle\!\rangle. \end{aligned} \tag{2.64}$$

The τ dependence drops out of the last term because Q and W commute.

To study ordering, it is of interest to investigate how S or χ grow with the system size. It turns out that a bound can be set to this. Let $\|M\|_\infty$ denote the matrix norm

$$\|M\|_\infty = \max_i |m_i| \tag{2.65}$$

where m_i are the eigenvalues of m_i. Clearly, for any $N \times N$ matrix M,

$$|\mathrm{Sp}\, M| \le N \|M\|_\infty . \tag{2.66}$$

Note that W satisfies

$$0 \le \|W\|_\infty \le 1, \tag{2.67}$$

and that $\mathrm{Sp}\, W = L\rho$, with ρ the density and L the number of lattice sites. Note that $0 \le \rho \le s$, where s is the spin multiplicity ($s = 1$ for spinless and $s = 2$ for spin–$\frac{1}{2}$ fermions), so that $\mathrm{Sp}\, \mathbb{1} = sL$.

Now, for correlations of the type (2.63), one easily derives that a bound is set by

$$|S_{c^\dagger A c,\, c^\dagger B c}| = \left|\langle\!\langle\, \mathrm{Sp}\, A^\dagger \cdot (\mathbb{1} - W) \cdot B \cdot W \,\rangle\!\rangle + \langle\!\langle\, \mathrm{Sp}\, A^\dagger \cdot W\, \mathrm{Sp}\, B \cdot W \,\rangle\!\rangle\right| \tag{2.68}$$

$$\le \langle\!\langle\, \left|\mathrm{Sp}\, A^\dagger \cdot (\mathbb{1} - W) \cdot B \cdot W\right| \,\rangle\!\rangle + \langle\!\langle\, \left|\mathrm{Sp}\, A^\dagger \cdot W\, \mathrm{Sp}\, B \cdot W\right| \,\rangle\!\rangle \tag{2.69}$$

$$\begin{aligned} &\le L \langle\!\langle\, \left\|A^\dagger \cdot (\mathbb{1} - W) \cdot B \cdot W\right\|_\infty \,\rangle\!\rangle + L^2 \langle\!\langle\, \left\|A^\dagger \cdot W\right\|_\infty \|B \cdot W\|_\infty \,\rangle\!\rangle \\ &\le sL \langle\!\langle\, \left\|A^\dagger\right\|_\infty \|B\|_\infty \,\rangle\!\rangle + (sL)^2 \langle\!\langle\, \left\|A^\dagger\right\|_\infty \|B\|_\infty \,\rangle\!\rangle \\ &= ((sL)^2 + sL) \langle\!\langle\, \left\|A^\dagger\right\|_\infty \,\rangle\!\rangle \langle\!\langle\, \|B\|_\infty \,\rangle\!\rangle. \end{aligned} \tag{2.70}$$

Thus, apart from an implicit L–dependence of A and B, this correlation can grow at most as L^2.

Similar bounds can be obtained for the susceptibilities (2.64), rather than the plain correlations, the integral accounting for an extra factor β.

Using the specific form of $W = (\mathbb{1} + \exp \beta Q)^{-1}$ for the GCE, the susceptibilities can be rewritten in a more explicit form. Diagonalizing Q explicitly with the orthogonal transformation

S, (2.64) gives

$$\begin{aligned}\chi_{\hat{A},\hat{B}} &= \left\langle\!\!\left\langle \sum_{ij} (S\cdot A^\dagger\cdot S^\dagger)_{ij}(S\cdot B\cdot S^\dagger)_{ij} \frac{1}{1+e^{-\beta\lambda_j}} \frac{1}{1+e^{\beta\lambda_i}} \int_0^\beta d\tau\, e^{\tau(\lambda_i-\lambda_j)} \right\rangle\!\!\right\rangle \\ &\quad + \beta \langle\!\langle \operatorname{Sp} A\cdot W \operatorname{Sp} B\cdot W \rangle\!\rangle. \\ &= \left\langle\!\!\left\langle \sum_{ij} (S\cdot A^\dagger\cdot S^\dagger)_{ij}(S\cdot B\cdot S^\dagger)_{ij} V_{ij}(\beta) \right\rangle\!\!\right\rangle + \beta \langle\!\langle \operatorname{Sp} A\cdot W \operatorname{Sp} B\cdot W \rangle\!\rangle, \end{aligned} \tag{2.71}$$

where

$$V_{ij}(\beta) = \frac{1}{1+e^{-\beta\lambda_j}} \frac{1}{1+e^{\beta\lambda_i}} \int_0^\beta d\tau e^{\tau(\lambda_i-\lambda_j)} \tag{2.72}$$

$$= \frac{\sinh \beta(\lambda_i-\lambda_j)/2}{2(\lambda_i-\lambda_j)\cosh \beta\lambda_i/2 \cosh \beta\lambda_j/2} \tag{2.73}$$

$$= \frac{\tanh \beta(\lambda_i-\lambda_j)/2}{(\lambda_i-\lambda_j)} \frac{\cosh \beta(\lambda_i-\lambda_j)/2}{\cosh \beta(\lambda_i-\lambda_j)/2 + \cosh \beta(\lambda_i+\lambda_j)/2} \leq \frac{\beta}{2}. \tag{2.74}$$

If we divide by β, this expression for V yields a stable way to compute at zero temperature: the first factor will tend to a delta function in $\lambda_i - \lambda_j$, whereas the second factor limits the contribution to terms ij with λ_i and λ_j around 0, ie. the Fermi surface. Thus to paraphrase sloppily: at low temperature, the major contribution to the response of an operator A to a disturbance of the system by an operator B comes from the convolution of states near the Fermi surface. This is of course a well known result (eg. [10]).

2.3.2 Correlations of pairing operators

In contrast to the above case of correlations of quadratic forms stands the case where $\hat{A}$ and $\hat{B}$ are of the form of pairing operators

$$\hat{A} = c\ \cdot A\cdot c\ , \qquad \hat{B} = c\ \cdot B\cdot c\ . \tag{2.75}$$

These pairing operators are relevant in the context of superconductivity, chapter 4. Application of equation (2.30) leads to

$$S_{\hat{A}\hat{B}} = \left\langle\, c^\dagger\cdot A^\dagger\cdot c^\dagger\ c\ \cdot B\cdot c\ \right\rangle = \langle\!\langle \operatorname{Sp} W\cdot A^\dagger\cdot W^\dagger\cdot (B - B^T) \rangle\!\rangle \tag{2.76}$$

so obviously

$$\begin{aligned} |S_{\hat{A}\hat{B}}| &\leq L\langle\!\langle \left\| W\cdot A^\dagger\cdot W^\dagger\cdot (B-B^T)\right\|_\infty \rangle\!\rangle \\ &\leq sL\langle\!\langle \|A\|_\infty \left\|B-B^T\right\|_\infty \rangle\!\rangle. \end{aligned} \tag{2.77}$$

In contrast with the previous case of quadratic forms, a term proportional to L^2 is absent, severely limiting the possibilities for orderings in the system associated with pairing operators like $c^\dagger\cdot A\cdot c^\dagger$. In chapter 4 this will be the basis of our argument that the class of models at hand cannot exhibit superconductivity.

For reference we give a similar formula as before for the susceptibility, useful in the numerical simulations.

$$\begin{aligned}
\chi_{\hat{A},\hat{B}} &= \int_0^\beta d\tau \Big\langle\, c^\dagger \cdot A^\dagger \cdot c^\dagger e^{-\tau c^\dagger \cdot Q \cdot c} c \;\cdot B \cdot c\; e^{\tau c^\dagger \cdot Q \cdot c} \,\Big\rangle \\
&= \int_0^\beta d\tau \Big\langle\, e^{\tau c^\dagger \cdot Q \cdot c} c^\dagger \cdot A^\dagger \cdot c^\dagger e^{-\tau c^\dagger \cdot Q \cdot c} c \;\cdot B \cdot c \,\Big\rangle \\
&= \int_0^\beta d\tau \big\langle\!\big\langle\, \mathrm{Sp}\, W \cdot e^{\tau Q} \cdot A^\dagger \cdot e^{\tau Q} \cdot W^\dagger \cdot (B - B^{\mathsf{T}}) \,\big\rangle\!\big\rangle \\
&= \Big\langle\!\Big\langle \sum_{ij} (S \cdot A^\dagger \cdot S^\dagger)_{ij} (S \cdot [B - B^{\mathsf{T}}] \cdot S^\dagger)_{ji} \frac{1}{1 + e^{\beta\lambda_j}} \frac{1}{1 + e^{\beta\lambda_i}} \int_0^\beta d\tau e^{\tau(\lambda_i + \lambda_j)} \Big\rangle\!\Big\rangle \\
&= \Big\langle\!\Big\langle \sum_{ij} (S \cdot A^\dagger \cdot S^\dagger)_{ij} (S \cdot B \cdot S^\dagger)_{ij} V'_{ij}(\beta) \Big\rangle\!\Big\rangle, \qquad (2.78)
\end{aligned}$$

with

$$\begin{aligned}
V'_{ij}(\beta) &= \frac{1}{1 + e^{\beta\lambda_j}} \frac{1}{1 + e^{\beta\lambda_i}} \int_0^\beta d\tau e^{\tau(\lambda_i + \lambda_j)} \qquad (2.79) \\
&= \frac{\sinh \beta(\lambda_i + \lambda_j)/2}{2(\lambda_i + \lambda_j) \cosh \beta\lambda_i/2 \cosh \beta\lambda_j/2} \qquad (2.80) \\
&= \frac{\tanh \beta(\lambda_i + \lambda_j)/2}{(\lambda_i + \lambda_j)} \frac{\cosh \beta(\lambda_i + \lambda_j)/2}{\cosh \beta(\lambda_i - \lambda_j)/2 + \cosh \beta(\lambda_i + \lambda_j)/2} \leq \frac{\beta}{2}. \qquad (2.81)
\end{aligned}$$

Note that (2.72) and (2.79) differ only in the sign preceding λ_j.

Specific correlations to be studied will be introduced in section 2.5, but first another technique to obtain useful information will be introduced.

2.3.3 Consistency equalities

By differentiation under the integral sign, using the symmetry of K,

$$Z^{-1} \int d\{x\} \frac{\partial}{\partial x} \mathrm{Tr}_f \exp\left\{-\beta \left(\tfrac{1}{2} x \bullet K \bullet x + x \bullet :c^\dagger \cdot \Lambda \cdot c: + :c^\dagger \cdot T \cdot c:\right)\right\} = -\beta \big\langle\, K \bullet x + :c^\dagger \cdot \Lambda \cdot c: \,\big\rangle, \qquad (2.82)$$

on the other hand

$$Z^{-1} \int d\{x\} \frac{\partial}{\partial x} \mathrm{Tr}_f \exp\left\{-\beta \left(\tfrac{1}{2} x \bullet K \bullet x + x \bullet :c^\dagger \cdot \Lambda \cdot c: + :c^\dagger \cdot T \cdot c:\right)\right\} = \Big[Z^{-1} \mathrm{Tr}_f \exp\left\{-\beta \left(\tfrac{1}{2} x \bullet K \bullet x + x \bullet :c^\dagger \cdot \Lambda \cdot c: + :c^\dagger \cdot T \cdot c:\right)\right\}\Big]_{x=-\infty}^{x=+\infty} = 0, \qquad (2.83)$$

on account of the negative quadratic leading term in the exponent. Hence

$$K \bullet \langle x \rangle = -\big\langle\, :c^\dagger \cdot \Lambda \cdot c: \,\big\rangle. \qquad (2.84)$$

By repeated differentiation under the integral a whole hierarchy of such equalities can be derived. Their importance lies in the fact that in a Monte Carlo simulation these equalities are *not* automatically satisfied, but can be checked quite easily. Thus they serve as a valuable check on the internal consistency of the simulation results.

2.4 Solvable cases of the Holstein model

The results covered in this chapter so far have been valid for all models satisfying property A (1.34). We will now restrict ourselves a bit further, to the Holstein model, specified by (1.23). For this case a few more analytic results are presented. Generalisations to less restricted models are either highly non–trivial or are not expected to bring much new insights. First the anti–integrable limit will be introduced for completeness. This is essentially the case $L = 1$. Then the case $L = 2$ for the adiabatic limit will be analysed in detail. Finally, the case of the half filled adiabatic limit will be presented.

2.4.1 The anti–integrable limit

In the limit of vanishing hopping t, systems satisfying property A+B such as the Holstein model become easily integrable as well. With the Λ^i diagonal with eigenvalues λ^i_j, the free energy separates into

$$F = -\beta^{-1} \log \mathrm{Tr} \prod_i \exp\left\{ -\beta \left[\frac{p_i^2}{2M} + \tfrac{1}{2} K x_i^2 + x_i \sum_j \lambda^i_j n_j \right] \right\} . \tag{2.85}$$

Completing the square in x_i, and performing the partial trace over the phonons gives

$$F = \sum_i F_{\mathrm{ph}}(K_i) - \beta^{-1} \log \sum_{\{n_i\}} \exp\left\{ \beta \sum_i \frac{1}{2K_i} \left(\sum_j \lambda^i_j n_j \right)^2 \right\} , \tag{2.86}$$

where $F_{\mathrm{ph}}(K)$ is the free energy of a free phonon with spring constant K. The second term is essentially an *attractive* Hubbard model in the atomic limit (vanishing hopping). It is immediately obvious that for any filling, the electrons will be distributed over the lattice so as to maximize the $(\sum_j \lambda^i_j n_j)^2$. Whatever the values of the λ^i_j, a doubly occupied site will contribute more than a singly occupied site, and so the ground state will be a distribution of localised bipolarons over the lattice, and may expected to be degenerate when the λ^i_j possess some regularity. Solving this problem is not harder than solving a classical lattice model (which may still be difficult).

This limit may serve as a starting point for perturbation theory in t, but in general this is not a good idea: due to the extreme degeneracy of the ground state, a subset of the ground state space may exhibit correlations that actually disappear immediately when $t \neq 0$[42].

2.4.2 The case $L = 2$

Consider now the adiabatic Holstein model with electrons of spin $\sigma = 0$ or $\sigma = \frac{1}{2}$. For a system of two lattice sites, the free energy (1.37) reduces to

$$F = -\beta^{-1} \log \iint dx_1 dx_2 \, \exp\left[-\tfrac{1}{2}\beta K \left(x_1^2 + x_2^2 \right) \right] \times \\ \times \det \left[2 \cosh \tfrac{1}{2}\beta \begin{pmatrix} \lambda x_1 - \mu & -t \\ -t & \lambda x_2 - \mu \end{pmatrix} \right]^s . \tag{2.87}$$

with $s = 2\sigma + 1$. Diagonalizing the 2×2 matrix explicitly, and transforming variables to

$$\nu = \tfrac{1}{2}\lambda(x_1 + x_2) - \mu, \qquad w = \tfrac{1}{2}\lambda(x_1 - x_2), \tag{2.88}$$

and dropping a constant term arising from the Jacobian, F can be written as

$$F = -\beta^{-1} \log \iint d\nu\, dw \exp\left[-\tfrac{1}{2}\beta \frac{K}{\lambda^2}\left(\nu^2 + w^2 + 2\mu\nu + \mu^2\right)\right] \times \\ \times \cosh^s[\tfrac{1}{2}\beta(\nu + \sqrt{w^2 + t^2})] \cosh^s[\tfrac{1}{2}\beta(\nu - \sqrt{w^2 + t^2})]. \tag{2.89}$$

This free energy, and the corresponding expectation values are readily evaluated using standard numerical integration procedures. However, we will just look at the ground state phase diagram as a function of the chemical potential μ and the coupling λ. This ground state is characterized by the ν and w which minimize the effective Hamiltonian

$$\mathcal{H}_{\text{eff}}(\nu, w) = \frac{K}{\lambda^2}(\nu^2 + w^2 + 2\mu\nu + \mu^2) \\ - s\beta^{-1} \log\cosh[\tfrac{1}{2}\beta(\nu + \sqrt{w^2 + t^2})] \cosh[\tfrac{1}{2}\beta(\nu - \sqrt{w^2 + t^2})]. \tag{2.90}$$

Equating the derivative with respect to ν to zero gives

$$U^{-1}(\nu + \mu) \quad = \quad \tanh[\tfrac{1}{2}\beta(\nu + \sqrt{w^2 + t^2})] + \tanh[\tfrac{1}{2}\beta(\nu - \sqrt{w^2 + t^2})] \tag{2.91}$$

where the effective interaction strength U appears,

$$U \quad \stackrel{\text{def}}{=} \quad \frac{s\lambda^2}{2K}. \tag{2.92}$$

Equating the derivative with respect to w to zero gives $w = 0$ or

$$U^{-1} \quad = \quad \frac{1}{2\sqrt{w^2 + t^2}} \left\{\tanh[\tfrac{1}{2}\beta(\nu + \sqrt{w^2 + t^2})] - \tanh[\tfrac{1}{2}\beta(\nu - \sqrt{w^2 + t^2})]\right\} \tag{2.93}$$

For the groundstate, $\beta \to \infty$, one has $\tanh \beta\alpha = \text{sign}\alpha$. Let us start at $\mu = 0$, then from symmetry, $\nu = 0$. The solution $w = 0$ of the latter equation will become unstable, and a second solution (and it's mirror image) will appear, if

$$U^{-1} \quad = \quad \frac{1}{\sqrt{w^2 + t^2}}. \tag{2.94}$$

This, in turn, can only happen when $U \geq t$. Suppose $U \leq t$, then if we change μ away from zero, the only way to satisfy the first equation is to have $\nu = -\mu$, until $\nu = \pm\sqrt{w^2 + t^2}$. Meanwhile, the second equation requires $w = 0$, until one of the $\tanh$ changes sign, so at $\nu = \pm t$. After this point, the first equation requires $\nu = -\mu \pm U$, depending on whether $\mu <> 0$.

Similarly, for $U \geq t$, if we change μ away from zero, the first equation will require $\nu = \mu$, but no $\tanh$ will change sign until $\nu = \pm\sqrt{w^2 + t^2} = \pm U^{-1} = -\mu$, after which the second equation *only* admits $w = 0$ as a solution. As w and ν are directly related to the 'dimerization' and the density, it is not difficult to complete the picture. An overview is given in figure 2-1. Note that, independent of the spin s, there is no phase with quarter or three quarter filling in the ground state.

As we will see in section 5.1, although a caricature, this picture covers the essential elements of the behaviour for any L.

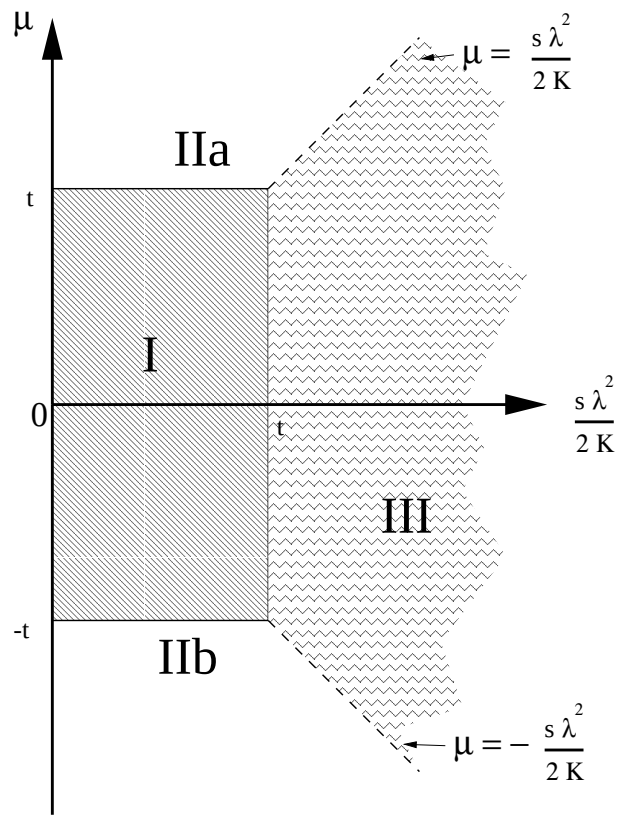

Figure 2-1: *The ground state phase diagram for the 2 site Holstein model (2.90).* $U = s\lambda^2/2K$ *is the effective coupling. Phase* **I**, *bounded by the rectangle* $(U, \mu) \in [0, t] \times [-t, t]$ *is half filled, with no dimerization and satisfies* $\nu = -\mu,\ w = 0$. *Phases* **IIa** *and* **IIb** *are completely filled, resp. empty, and undimerized and satisfy* $\nu = -\mu \pm \frac{1}{2}U,\ \ w = 0$. *Phase* **III** *is half filled and dimerized with* $\nu = -\mu,\ w = \pm\sqrt{U^2 - t^2}$.

2.4.3 The Peierls trial state

In the adiabatic limit, finding the groundstate is equivalent to finding the configuration $\{x_i\}$ that minimizes the effective Hamiltonian $\mathcal{H}_{\text{eff}}(\{x_i\})$ for $\beta \to \infty$. Although it is in general impossible to do this in closed form, one may guess a subspace of the configuration space in which the minimum is to be found, for which the effective Hamiltonian and its derivatives may be calculated and solved explicitly. The most obvious example, given the result for $L = 2$, would be the case of half filling for the Holstein Model in one dimension with spin σ. Again, let $s = 2\sigma + 1$. Construct a staggered trial state

$$x_i = \bar{x} + (-)^i \tilde{x}, \tag{2.95}$$

then from (2.84) we know that $K \sum_i x_i = \lambda L(\rho - 1) = 0$, so $\bar{x} = 0$, and we put

$$L^{-1}\mathcal{H}_{\text{eff}}(\tilde{x}) = \tfrac{1}{2}K\tilde{x}^2 - \frac{s}{Lb}\log\det 2\cosh\tfrac{1}{2}\beta(T + \lambda\tilde{x}\,\mathrm{diag}(-1)^i), \tag{2.96}$$

where $\mathrm{diag}(-1)^i$ denotes the matrix with alternately $+1, -1$ on the diagonal. The eigenvalue problem for $T + \lambda\tilde{x}\,\mathrm{diag}(-1)^i$ is easily solved (by Fourier transformation of its square) to yield

$$L^{-1}\mathcal{H}_{\text{eff}}(\tilde{x}) = \tfrac{1}{2}K\tilde{x}^2 - \frac{s}{L\beta}\sum_{k=0}^{L-1}\log 2\cosh\tfrac{1}{2}\beta\sqrt{(\lambda\tilde{x})^2 + (2t\cos 2\pi k/L)^2}. \tag{2.97}$$

We may now wonder under which conditions there exists a $\tilde{x} \neq 0$ that minimizes this expression. The answer depends rather subtly on the order in which we differentiate and take the limits $x \to 0$, $L \to \infty$ and $\beta \to \infty$.

In (2.97) the limit $\beta \to \infty$ can be taken without complications, with the result

$$\begin{aligned} L^{-1}\mathcal{H}_{\text{eff}}(\tilde{x}) &= \tfrac{1}{2}K\tilde{x}^2 - \frac{s}{2L}\sum_{k=0}^{L-1}\sqrt{(\lambda\tilde{x})^2 + (2t\cos 2\pi k/L)^2} \\ &= \tfrac{1}{2}K\tilde{x}^2 - \tfrac{1}{2}s\sqrt{(\lambda\tilde{x})^2 + (2t)^2}\,\mathcal{E}_L(\alpha) \end{aligned} \tag{2.98}$$

where

$$\begin{aligned} \alpha &= \frac{(2t)^2}{(2t)^2 + (\lambda\tilde{x})^2}. \\ \mathcal{E}_L(\alpha) &= \frac{1}{L}\sum_{k=0}^{L-1}\sqrt{1 - \alpha\sin^2 2\pi k/L}. \end{aligned} \tag{2.99}$$

This function $\mathcal{E}_L(\alpha)$ may be considered a "finite–L" approximant to the complete elliptic integral of the second kind,

$$\mathcal{E}(\alpha) \overset{\text{def}}{=} \frac{1}{2\pi}\int_0^{2\pi}\sqrt{1 - \alpha\sin^2 k}\,dk. \tag{2.100}$$

For $0 \leq \alpha \leq 1$ this is well defined and and hence for any $\tilde{x}$ (2.98) can be evaluated numerically to any desired precision.

Introducing $\Delta = \lambda\tilde{x}/2t$, and with $U = s\lambda^2/2K$ like before, we can reformulate the problem as finding the Δ which minimizes

$$\frac{\mathcal{H}_{\text{eff}}}{Lst} = \frac{t\Delta^2}{U} - \sqrt{1 + \Delta^2}\,\mathcal{E}_L\left(\frac{1}{1 + \Delta^2}\right). \tag{2.101}$$

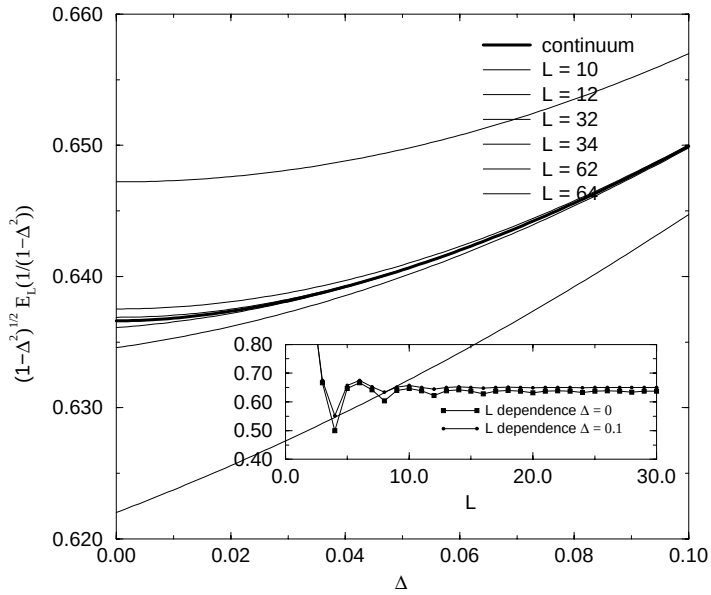

Figure 2-2: *The second term of (2.101) as a function of the gap* Δ *and system size* L.

Figure 2-2 shows the second term as a functions of Δ and L. Two facts strike the eye: the finite–L approximations alternate around the integral expression, with convergence worsening for $\Delta \to 0$. Secondly, for L divisible[2] by 4, the first derivative of the finite–L approximation does not seem to vanish. This means that for $L :: 4$, there will *always* be a solution $\Delta \neq 0$ minimizing (2.101), although this solution will vanish like $1/L$ for large L.

If we try to evaluate the derivatives of (2.101), the square root spoils the day: The function is not analytic at $\Delta = 0$, ie. it need not converge to its Taylor series. Consider the first derivative of (2.101),

$$\frac{\partial}{\partial\Delta}\frac{\mathcal{H}_{\text{eff}}}{Lst} = \frac{2t\Delta}{U} - \frac{\Delta}{\sqrt{1+\Delta^2}}\mathcal{K}_L\left(\frac{1}{1+\Delta^2}\right), \tag{2.102}$$

with

$$\mathcal{K}_L(\alpha) = \frac{1}{L}\sum_{k=0}^{L-1}\frac{1}{\sqrt{1-\alpha\sin^2 2\pi k/L}}, \tag{2.103}$$

which analogously can be considered a finite–L approximant to the complete elliptic integral of the first kind

$$\mathcal{K}(\alpha) \stackrel{\text{def}}{=} \frac{1}{2\pi}\int_0^{2\pi}\frac{dk}{\sqrt{1-\alpha\sin^2 k}}. \tag{2.104}$$

[2] henceforth abbreviated as $L :: 4$.

For $\alpha \to 0$ this approaches unity, giving rise to the strong coupling limit solution

$$\Delta \;=\; \frac{U}{2t}. \tag{2.105}$$

On the other hand, for $\alpha \to 1$, $\mathcal{K}$ diverges logarithmically,

$$\lim_{\alpha\to 1}\left[\mathcal{K}(\alpha) - \frac{1}{\pi}\log\frac{16}{1-\alpha}\right] \;=\; 0 \tag{2.106}$$

therefore, in the limit $\Delta \to 0$,

$$\frac{\partial}{\partial\Delta}\frac{\mathcal{H}_{\text{eff}}}{Lst} \;\to\; \frac{2t\Delta}{U} + \frac{\Delta}{\pi\sqrt{1+\Delta^2}}\left[\log 16 - 2\log\Delta + \log 1+\Delta^2\right] \to 0. \tag{2.107}$$

Equating this to zero it follows that for small U/t, ie. for small coupling

$$\lim_{U/t\to 0}\Delta_0 = 4e^{-\pi t/U}. \tag{2.108}$$

This means that (even for infinite L) we always have a dimerization, but for small couplings it vanishes exponentially. This argument is known in the literature as the Peierls argument[10, 18], so it is reasonable to call the state characterised by (2.95), the Peierls trial state.

We can now understand the finite–L behaviour in terms of the above analysis. If L is divisible by 4, the sum in (2.97) will contain a term

$$L^{-1}\log 2\cosh\tfrac{1}{2}\beta\lambda\tilde{x}$$

whose derivative with respect to $\tilde{x}$ will diverge with β. This gives rise to a non–vanishing solution for $\tilde{x}$, which, decreases with L until the infinite L value is reached. For L not divisible by 4, there will be a critical coupling, depending on L, below which the gap induced by the dimerization is smaller than the finite–size effect gap, which is equal to the spacing of the eigenvalues, eg. for a half filled 1–d system

$$\Delta_{fs} \;=\; 4t\sin 2\pi/L, \tag{2.109}$$

so there will be an artificial transition for $\Delta_0 = \Delta_{fs}$, ie.

$$e^{-\pi t/U} = t\sin 2\pi/L. \tag{2.110}$$

This finite size effect of having a gap proportional to $1/L$ will also make itself felt when the temperature is increased. We may expect the signs of a 'transition' to appear when the temperature becomes of the order of this gap.

Note that strictly speaking, all of the above does not constitute a proof that the actual groundstate is dimerized or not. Kennedy and Lieb[51, 63] have shown that under sufficiently general conditions, in one dimension at half filling no other *periodic* state can have a lower energy than the dimerized state (which has a period of two lattice sites).

The energy that we get from the Peierls trial state is an upper bound to the upper bound (2.55), which may be compared to other upper bounds, like the one from BCS theory that will be treated in chapter 4. This will be done in sections 4.4 and 5.1.3.

2.5 Numerical simulation with the effective Hamiltonian

The adiabatic limit as introduced in section 2.1 is suitable for very accurate and fast numerical simulations[27, 38]. This section will be devoted to the exposition of the method. First, the Metropolis Monte Carlo method of section 1.3 is applied to evaluate the average denoted by $\langle\!\langle \ldots \rangle\!\rangle$, equation (2.15). Alternatively, a conjugate gradient method can be applied to get results for zero temperature.

In consequent sections, a number of relevant and interesting quantities, among which the static correlation functions, are expressed in terms of the matrix $W_{ij} = \overline{c_j^\dagger c_i}$, equation (2.16). As an example we will consider some results of the simulation of the simplest model in the class of models under consideration: the spin-$\frac{1}{2}$ Holstein model with nearest neighbour hopping (1.23) in the adiabatic limit. In particle–hole symmetric form:

$$\mathcal{H}_{ad} = \frac{K}{2}\sum_i x_i^2 + \sum_i (\lambda x_i - \mu)(n_i - 1) + :c^\dagger \cdot T_0(t) \cdot c:, \tag{2.111}$$

with T_0 like (1.5) and spin-$\frac{1}{2}$ so $n_i = n_{i\uparrow} + n_{i\downarrow}$. In section 2.5.6 the results for a one dimensional system at half filling will be compared to the treatment of section 2.4.3 and the literature. In all cases we apply periodic boundary conditions on the lattice. A more thorough exploration of the phase diagram is postponed to chapter 5, when the dynamic correlations and superconductivity will have been introduced.

In all graphs in this section, the lines that connect the data points are but guides to the eye.

2.5.1 Metropolis Monte Carlo

The effective Hamiltonian $\mathcal{H}_{eff}(x)$, equation (2.12) can be plugged into the MMCStep algorithm of section 1.3 directly, provided we can evaluate the Canonical or Grand Canonical expression for $-\beta^{-1}\log Z_f$. Because $\mathcal{H}_{eff}$ is a real number, the weights in the MMC algorithm are strictly positive, and no special tricks have to be invented to get around the so–called sign problem of Quantum Monte Carlo. In this sense too $\mathcal{H}_{eff}$ is a classical Hamiltonian, albeit with complicated interactions. Evaluation of $-\beta^{-1}\log Z_f$ in turn is feasible because we just need to construct $Q(x)$ and find its eigenvalues. The idea to decompose the thermodynamical average into a fermionic part that could be done analytically and a Monte Carlo over remaining degrees of freedom first appeared in Michielsen *et.al.* (1992)[27], where it was applied to the Montorsi–Rassetti Model, in which the remaining degrees of freedom are not adiabatic phonons but "frozen" fermions.

Because Q is block diagonal in the spin structure, and in fact, $Q_{\uparrow\uparrow} = Q_{\downarrow\downarrow}$ in the absence of a magnetic field, a lot of time can be saved at the expense of the appearance of a lot of factors 2 in all sorts of expressions. Once the eigenvalues are known care must be taken to avoid overflow for large inverse temperature β, but otherwise evaluation of (2.11) or (2.34) is straightforward.

The program for the Monte Carlo simulation of (1.3) used comes in two versions: one for finite β, with special care taken to correctly evaluate expressions for large β, and one in which in all expressions the limit $\beta \to \infty$ has been taken. In this limit, the Metropolis Monte Carlo algorithm becomes nothing but a very expensive trial and error method. Setting $\beta t = 10^4$ in the finite-β version yields results indistinguishable from the infinite β (ie. true groundstate) case.

For more than two particles, the loops over the determinant in the Canonical simulation become too elaborate to allow for large lattices, so we have to restrict ourselves to one particle (or hole) simulation in the Canonical ensemble, or Grand Canonical simulations. Two particle simulations n the Canonical ensemble are feasible but will not be considered here. At half–filling, ie. $\rho = s/2$ (s the spin multiplicity), we need to use the GCE. Using the particle–hole symmetric form we know that we must put $\mu = 0$ to get $\rho = s/2$. Occasionaly, this does not happen, and the simulation apparently gets stuck in some local minimum in phase space. Making other runs with the same parameters is the only check, as such local minima can be distinguished from the ground state by their total energy. For other densities the chemical potential μ has to be tuned, which can take considerable effort.

Trial configurations x are generated by making a 'small step' δx in configuration space. This can be done either in real or in reciprocal space, ie. by adding a random number to a randomly chosen component of the vector x, or by adding a cosine with random amplitude and random phase and wavelength to the entire vector. In either case it is essential that the average size of the steps can be tuned, so that the acceptance rate of the MMCStep fluctuates around 50%. Other methods of generating trial configurations may be found, but if their step size is not tunable, in general the energy differences in (1.51) will be too large ever to be accepted by the algorithm when the temperature is lowered. For the Holstein model, this step size is approximately independent of couplings and system size, and increases with the square root of the temperature. Knowing this saves a lot of fiddling with the parameters

A sequence of L (the number of lattice sites) MMCStep-s is called an MMCSweep. After some number of sweeps to bring the system to equilibrium the 'measurements' are started in which all quantities of interest, introduced below, are sampled after every MMCSweep. Many of these depend on $W(x)$, so the first step in a measurement is to diagonalize Q again. This time not only the eigenvalues ε_i but also the ortogonal transform S is obtained. As W is an algebraic function of Q, S diagonalizes Q as well.

Finding the eigenvalues of Q can be done in at most $\mathcal{O}(L^3)$ CPU–time. Because the measurements treated in this section consume at most $\mathcal{O}(L^3)$ CPU time too, the entire simulation program runs in $\mathcal{O}(L^3)$ time per sweep, so $\mathcal{O}(L^4)$ in total. See figure 2-3.

The results shown in this section are in units $K = t = 1$ of (2.111), at a scaled inverse temperature $\beta t = 10^4$. Production data for all results presented in this work were obtained by making 200 equilibration Monte Carlo sweeps followed by another 200 in which the measurements took place. The total energy is monitored during the equilibration phase of the simulation, to check if equilibrium has been attained, which is indicated by reaching a plateau. Occasionaly runs with 2000+2000 sweeps were used to check the results.

2.5.2 Conjugate gradient minimization

When $\mathcal{H}_{\text{eff}}$ and its derivatives are known, in principle we could follow the gradient in the energy landscape to walk down to a (local) minimum, which is a candidate for the groundstate. A better way than this Steepest Descent Method is called the Conjugate Gradient Method which avoids spurious detours in narrow valleys. For a clear exposition of this method we refer to the literature[16]. Here it suffices to say that once subroutines exists to calculate the energy $\mathcal{H}_{\text{eff}}$ and the force vector $-\partial\mathcal{H}_{\text{eff}}/\partial x_i$, these can be called by a library routine that iteratively finds a (possibly local) minimum. Initializing with a suitably drawn random state one can find various local minima that can be compared in energy and character to gain information on the ground state.

That the force vector can be calculated with little more effort than the energy itself follows

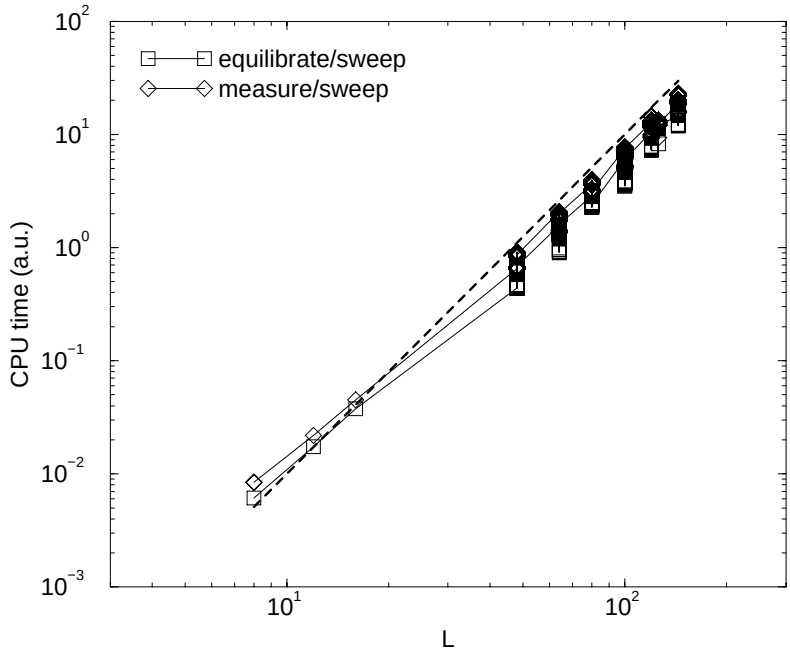

Figure 2-3: *CPU time consumption per MMCSweep (arbitrary units) for different system sizes. For a particular version of the GCE/Holstein MMC code these are the times per sweep of the equilibration and measurement phase, according to* `times(3)`*. The dashed line is the curve time* $\sim \mathrm{L}^3$*. Typical times for a 200–200 MMC–sample run on a single processor of the Cray J932 were around 80 CPU minutes for 126 lattice sites and 5 CPU seconds for 10 sites.*

from simply differentiating (2.12):

$$\frac{\partial \mathcal{H}_{\text{eff}}}{\partial x_i} = (K \bullet x)_i + \mathrm{Sp}\, W \cdot \Lambda^i. \tag{2.112}$$

Hence, diagonalizing Q to find its eigenvalues and the orthogonal transformation S yields sufficient information to do the trick. Note that W depends on β, so that the limit $\beta \to \infty$ still has to be taken.

2.5.3 Symmetries and uniqueness of the groundstate

The description of the system in terms of an electronic subsystem parametrized by a classical field x brings about an important question: Will a groundstate found by zero–temperature MMC or by CGM be unique? In the case of half filling, as treated in section 2.4.3 the answer clearly is negative. This is due to symmetry: for even L there are two configurations. With periodic boundary conditions (all cases treated in this thesis) and coupling matrices Λ homogeneous in all indices and homogeneous hopping T, a discrete displacement over the lattice is always such a symmetry. In general two configurations that are related by a symmetry of the Hamiltonian will be separated by tremendous energy barriers for the MMC loop. Thus, the measurement may exhibit a 'spontaneously broken' symmetry. Although this may be *related* to the question of ergodicity in statistical mechanics, it is *due* to lack of ergodicity of the MMC trajectory. It is important to re–symmetrize such measurements before concluding a certain ordering is present. In other words: it does not make sense to measure a quantity that does not obey a symmetry of the system.

2.5.4 Static correlations

Densities in real and reciprocal space

The first quantity of interest is the density. In the Grand Canonical simulation μ is specified, and ρ is obtained in the simulation. In Canonical simulations this is a (hopefully superfluous) check on the consistency of the program. Clearly,

$$\rho = \frac{1}{L}\left\langle \sum_i c_i^\dagger c_i \right\rangle = \frac{1}{L}\sum_i \langle\langle W_{ii} \rangle\rangle = \frac{1}{L}\,\mathrm{Sp}\,\langle\langle W \rangle\rangle. \tag{2.113}$$

The terms W_{ii} under the summation are of course just the local electron density at site $\vec{\imath}$ modulo the spin dependence. We mentioned that in case of a particle–hole symmetric Hamiltonian $\rho = s/2$ for $\mu = 0$.

Fourier transforming the spatial parts of the indices of W we obtain the distribution of the electrons in momentum space:

$$\left\langle n_\sigma(\vec{k}) \right\rangle = \frac{1}{L}\sum_{\vec{i}\vec{j}} e^{i\vec{k}\cdot(\vec{i}-\vec{j})} \left\langle\left\langle W_{\vec{i}\sigma,\vec{j}\sigma} \right\rangle\right\rangle. \tag{2.114}$$

In traditional treatments of infinite lattice systems with built–in translational invariance, the momentum representation is considered to be more appropriate, as the eigenstates of the Hamiltonian are supposed to be eigenstates of momentum operator. In that respect, the current treatment is more general, as no such assumptions went in to the derivations so far. Hence the methods may be applied to finite-L molecules or mesoscopic clusters.

Terms of the Hamiltonian

The respective terms in the Hamiltonian are compactly expressed as

$$\langle \mathcal{H}_{\mathsf{ph}} \rangle = \tfrac{1}{2}\langle\!\langle\, x \bullet K \bullet x \,\rangle\!\rangle = \tfrac{1}{2}\sum_{ij} K_{ij}\langle\!\langle\, x_i x_j \,\rangle\!\rangle \tag{2.115}$$

$$\langle \mathcal{H}_{\mathsf{el}} \rangle = \mathrm{Sp}\,\langle\!\langle\, W \cdot T \,\rangle\!\rangle = \mathrm{Sp}\,\langle\!\langle\, W \,\rangle\!\rangle \cdot T \tag{2.116}$$

$$\langle \mathcal{H}_{\mathsf{int}} \rangle = \langle\!\langle\, x \bullet \mathrm{Sp}\, W \cdot \Lambda \,\rangle\!\rangle_{\cdot} = \sum_i \left\langle\!\!\left\langle\, x_i (\mathrm{Sp}\, W \cdot \Lambda^i) \,\right\rangle\!\!\right\rangle_{\cdot}. \tag{2.117}$$

The alternative expressions listed differ only in the order of the summations. Note that anything that cannot be taken out of the $\langle\!\langle \ldots \rangle\!\rangle$ *has* to be evaluated inside the MMC loop, which is costly in terms of CPU time. Therefore the last expressions listed are the ones actually used. With a Sp inside the MMC loop, $\mathcal{H}_{\mathsf{int}}$ is an exception: because the Λ^i are (usually) sparse this Sp is only $\mathcal{O}(L)$ we can eliminate storage to an L^3 array in memory by evaluating it inside the loop.

The expectation value of the sum of the three terms in the Hamiltonian, ie. the total energy E_{total} is plotted for the half–filled 1–d system at zero temperature in figure 2-4. No meaningful differences are found between the MMC and CGM results and the Peierls–treatment of section 2.4.3. Also the bounds (2.57) are shown for $\hbar\omega = 0.5$.

Spatial ordering

As remarked, static correlation functions are useful in detecting *ordering* in the thermodynamic state. A first indication of whether the electrons behave in a correlated way is given by the double occupancy, defined by

$$P_2 \stackrel{\mathrm{def}}{=} \frac{1}{L}\sum_{\vec{l}} \left\langle\, n_{\vec{l}\uparrow} n_{\vec{l}\downarrow} \,\right\rangle = \frac{1}{L}\sum_{\vec{l}} \left\langle\!\!\left\langle\, W_{\vec{l}\uparrow,\vec{l}\uparrow} W_{\vec{l}\downarrow,\vec{l}\downarrow} \,\right\rangle\!\!\right\rangle. \tag{2.118}$$

This measures the extent to which sites are doubly occupied.

The Charge and Spin Density (CD and SD) correlation functions provide more detailed information about the distribution of charge (proportional to $n_{\vec{i}\uparrow} + n_{\vec{i}\downarrow}$) and spin (proportional to $n_{\vec{i}\uparrow} - n_{\vec{i}\downarrow}$) over the lattice sites $\vec{i}$. They are defined by

$$S^{\mathsf{cd}}_{\vec{i}\vec{j}} = \left\langle\, (n_{\vec{i}\uparrow} + n_{\vec{i}\downarrow})(n_{\vec{j}\uparrow} + n_{\vec{j}\downarrow}) \,\right\rangle \tag{2.119}$$

$$S^{\mathsf{sd}}_{\vec{i}\vec{j}} = \left\langle\, (n_{\vec{i}\uparrow} - n_{\vec{i}\downarrow})(n_{\vec{j}\uparrow} - n_{\vec{j}\downarrow}) \,\right\rangle, \tag{2.120}$$

and can conveniently be expressed and calculated as in section 2.3, when we make the spin index explicit and introduce the auxiliary operators $C_{\vec{i}}$ and $S_{\vec{i}}$ as

$$n_{\vec{i}\uparrow} + n_{\vec{i}\downarrow} = c^\dagger \cdot C_i \cdot c \tag{2.121}$$

$$n_{i\uparrow} - n_{i\downarrow} = c^\dagger \cdot S_i \cdot c \tag{2.122}$$

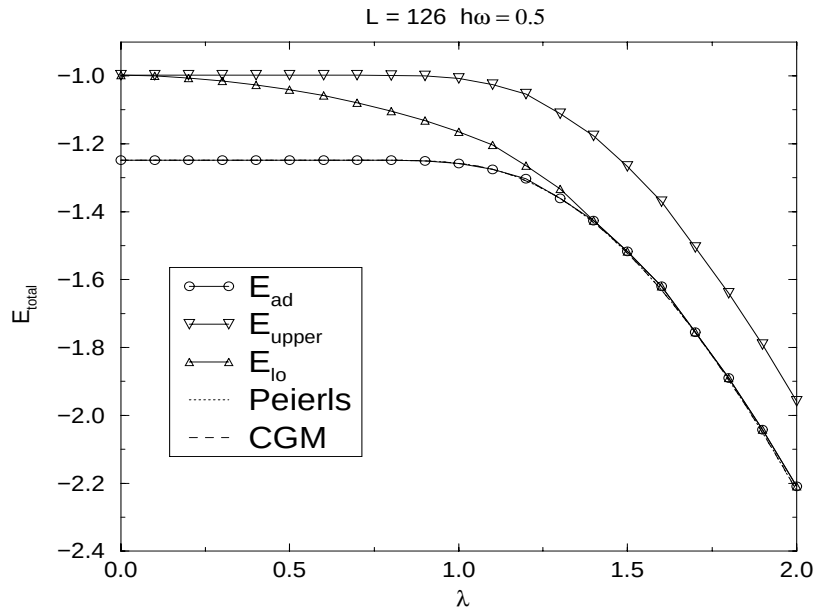

Figure 2-4: *Bounds to the ground state energy* E_{total} *for the Holstein model at half filling in 1 dimension. The zero–temperature MMC simulation with* $\mathrm{L} = 126$ *gives an* E_{ad} *(*$\circ$*), which is indistinguishable from the CGM and Peierls (solid lines) results. The upper bound (2.55) (*$\bigtriangledown$*) and the better lower bound (2.50) (*$\bigtriangleup$*) are derived from the MMC–*E_{ad} *with* $\hbar\omega = 0.5$.

Then equation (2.63) can be used to yield

$$S^{cd}_{i\vec{j}} = \langle\, c^\dagger \cdot C_i \cdot c\, c^\dagger \cdot C_j \cdot c \,\rangle \tag{2.123}$$

$$= \sum_\sigma \left\langle\!\!\left\langle\, (\delta_{\vec{i}\vec{j}} - W_{\vec{i}\sigma,\vec{j}\sigma}) W_{\vec{j}\sigma,\vec{i}\sigma} \,\right\rangle\!\!\right\rangle + \left\langle\!\!\left\langle\, (W_{\vec{i}\uparrow,\vec{i}\uparrow} + W_{\vec{i}\downarrow,\vec{i}\downarrow})(W_{\vec{j}\uparrow,\vec{j}\uparrow} + W_{\vec{j}\downarrow,\vec{j}\downarrow}) \,\right\rangle\!\!\right\rangle, \tag{2.124}$$

$$S^{sd}_{i\vec{j}} = \langle\, c^\dagger \cdot S_i \cdot c\, c^\dagger \cdot S_j \cdot c \,\rangle \tag{2.125}$$

$$= \sum_\sigma \left\langle\!\!\left\langle\, (\delta_{\vec{i}\vec{j}} - W_{\vec{i}\sigma,\vec{j}\sigma}) W_{\vec{j}\sigma,\vec{i}\sigma} \,\right\rangle\!\!\right\rangle + \left\langle\!\!\left\langle\, (W_{\vec{i}\uparrow,\vec{i}\uparrow} - W_{\vec{i}\downarrow,\vec{i}\downarrow})(W_{\vec{j}\uparrow,\vec{j}\uparrow} - W_{\vec{j}\downarrow,\vec{j}\downarrow}) \,\right\rangle\!\!\right\rangle. \tag{2.126}$$

With the assumption that $W_{\uparrow\uparrow} = W_{\downarrow\downarrow}$, eg. in the absence of magnetic fields, the last term of S^{sd} vanishes. Using translational invariance, these matrices too are transformed to reciprocal space, using

$$S^{cd}(q) = L^{-1} \sum_{ij} e^{2\pi i \vec{q}\cdot(\vec{i}-\vec{j})} S^{cd}_{i\vec{j}} \tag{2.127}$$

and likewise for the Spin Density correlations.

These correlations are illustrated for the example system in figure 2-5. Clearly a Charge Density Wave with wavenumber $k = \pi$ is present for large enough coupling, whereas for other wavelengths or in the Spin Density (fig. 2-6) no such signal is found.

In a similar way, the correlations between the phonons are handled to detect ordering in these degrees of freedom.

$$X_q \stackrel{def}{=} L^{-1} \sum_{ij} e^{2\pi i \vec{q}\cdot(\vec{i}-\vec{j})} \langle\!\langle\, x_i x_j \,\rangle\!\rangle. \tag{2.128}$$

With the bounds of section 2.3 one checks that these correlations in reciprocal space, $S^{cd}(q)$, $S^{sd}(q)$ and $X(q)$ can grow at most linearly with the system size L. It is instructive to compare $\langle\, xx \,\rangle$ to $\langle\, x \,\rangle\langle\, x \,\rangle$ (figures 2-7 an 2-8). Well away from the ordering transition these two are equal, but in the neighbourhood of the transition their difference, which measures the fluctuation increases. This is a useful method to pinpoint transitions in numerical situations.

The staggered Peierls trial state of section 2.4.3 has the correlation $X_{\pi/2}$ growing linear with L. Using the consistency equalities of section 2.3.3 it immediately follows that a Charge Density wave of wavenumber $\pi/2$ exists simultaneously with such an ordered state of the phonons. This behaviour can be checked at half filling, see figure 2-9: if the trial state is any good, the low–temperature Monte Carlo simulation should produce the same correlations. It turns out that this *is* the case. This also suggests that we should look for similar correlations with wavenumbers proportional to the filling factor for non half–filled systems.

2.5.5 The density of states

The single particle Density of States is an important quantity, being directly related to photo emission spectroscopy (PES), and simultaneously of fundamental importance in understanding the electronic structure of a system.

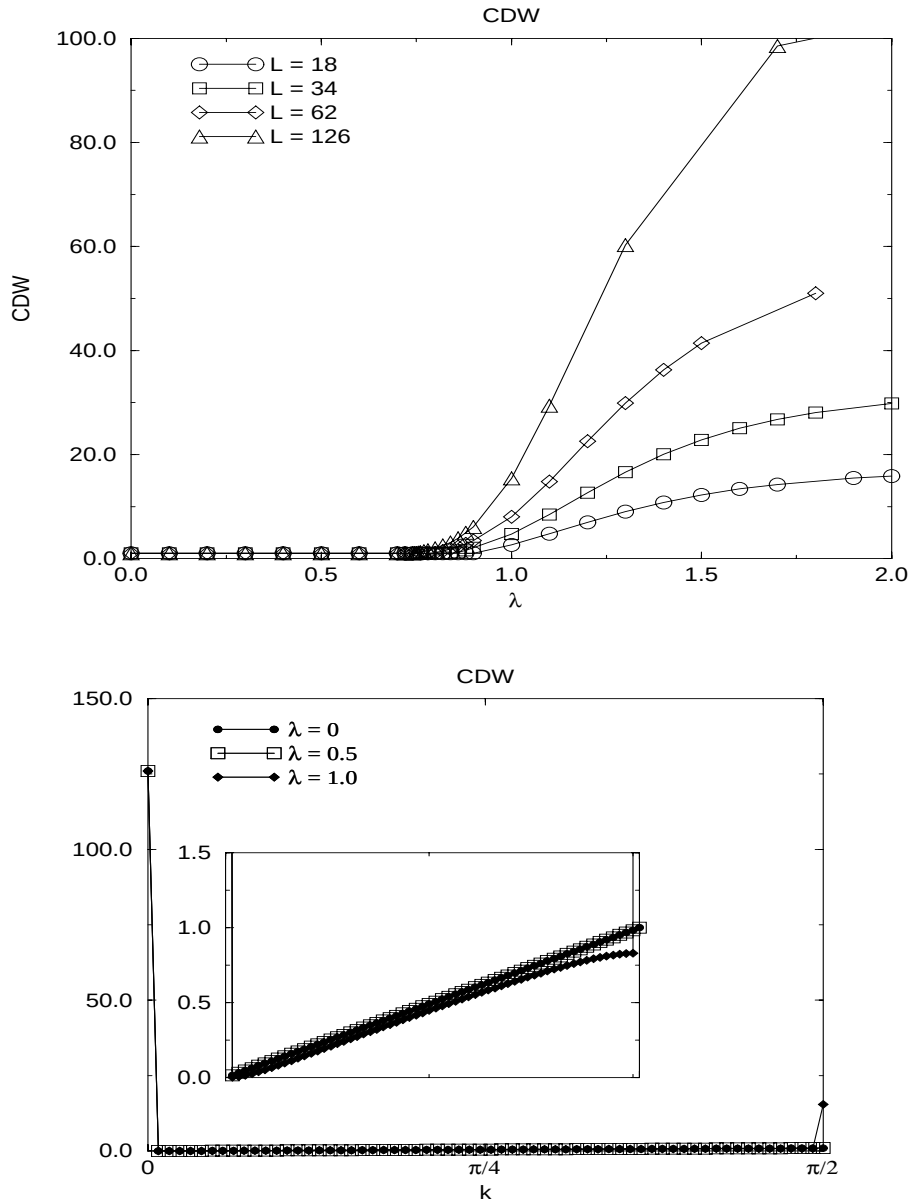

Figure 2-5: *Charge Density Wave correlations for* $T = 0,\ \rho = 1$ *in 1 dimension as a function of the coupling* λ *(top) and as a function of wave vector* k *(bottom). As the peaks in the CDW for* $k = 0$ *and* $k = \pi$ *are rather dominant, the inset shows the same graph on a different scale.*

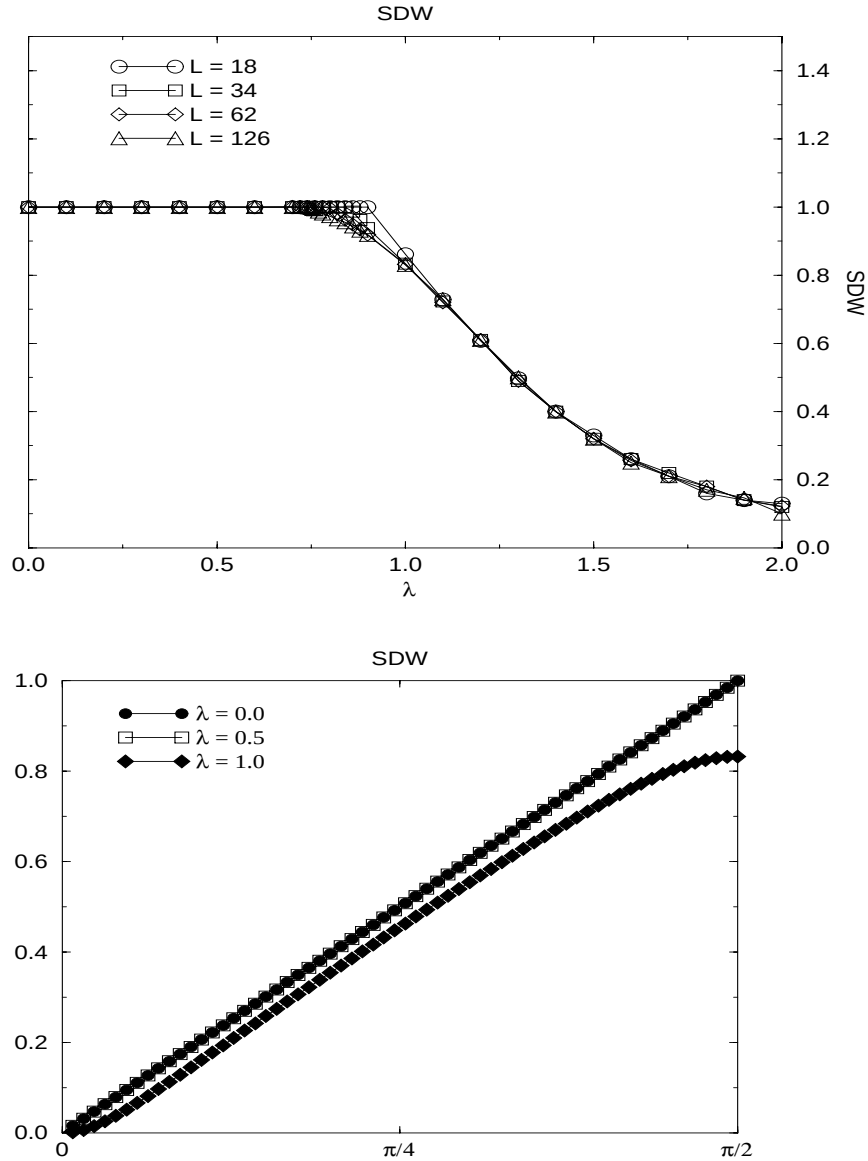

Figure 2-6: *Spin Density Wave correlations for* $T = 0,\ \rho = 1$ *in 1 dimension as a function of the coupling* λ *(top) and as a function of wave vector* k *(bottom). In contrast to the CDW shown in fig. 2-5 the SDW does not significantly vary with the system size* L.

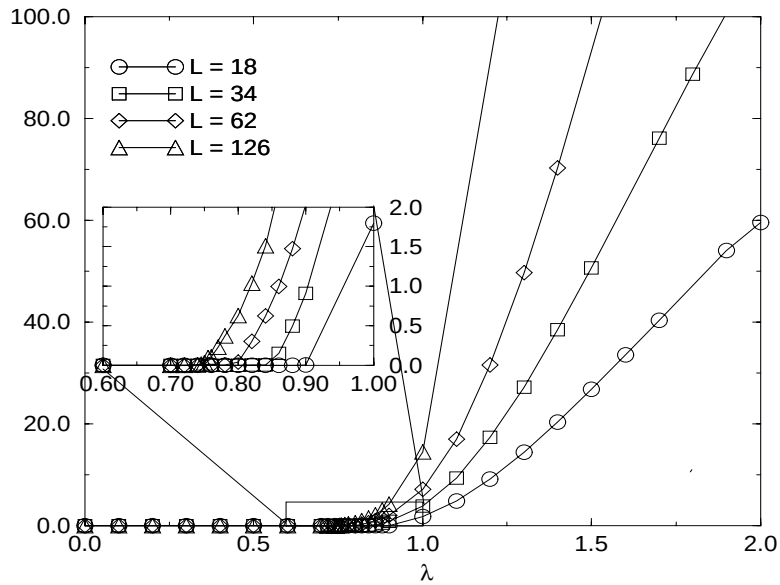

Figure 2-7: *Dimerization correlations*($k = \pi$) *for* $T = 0$, $\rho = 1$ *in 1 dimension,* $\langle xx \rangle$ *as a function of the coupling* λ *for various system sizes.*

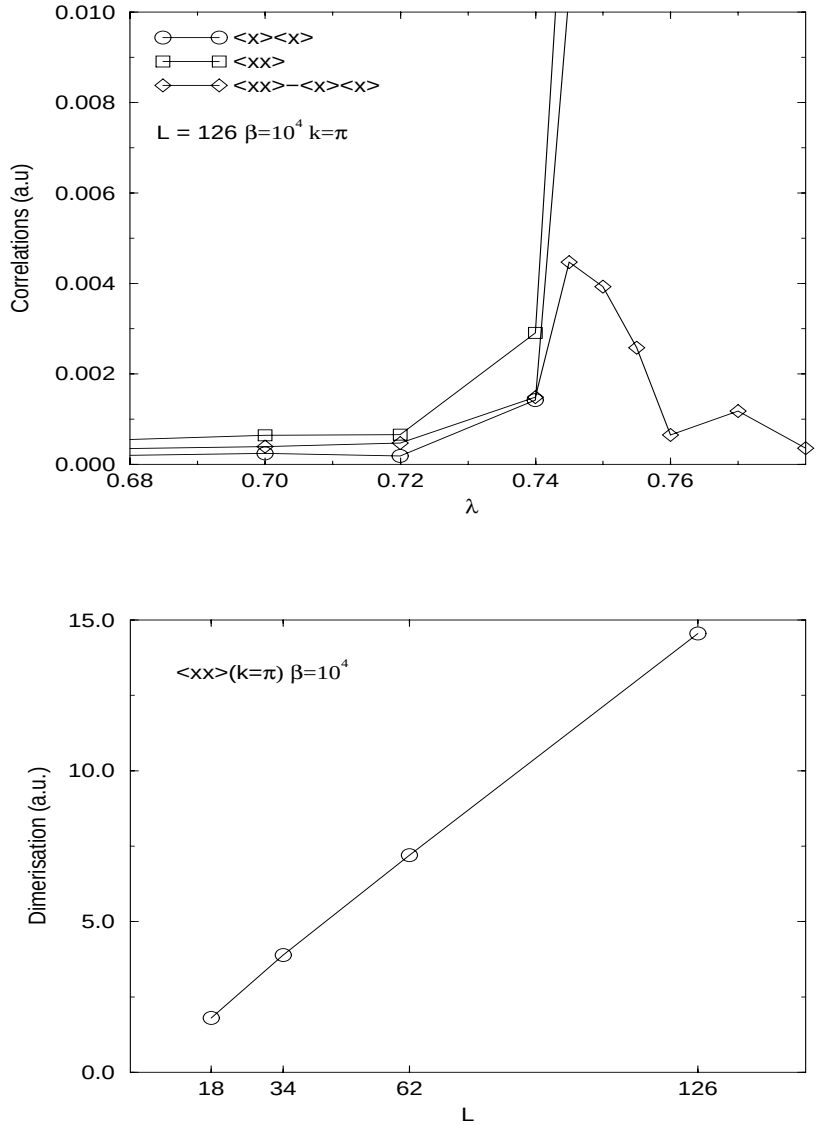

Figure 2-8: *Dimerization correlations*($k = \pi$) *for* $T = 0$, $\rho = 1$ *in 1 dimension. Top: comparison of* $\langle x \rangle \langle x \rangle$, $\langle xx \rangle$ *and their difference as a function of the coupling* λ *for* $L = 126$. *Bottom:* $\langle xx \rangle$ *as a function of system size for* $\lambda = 1.0$.

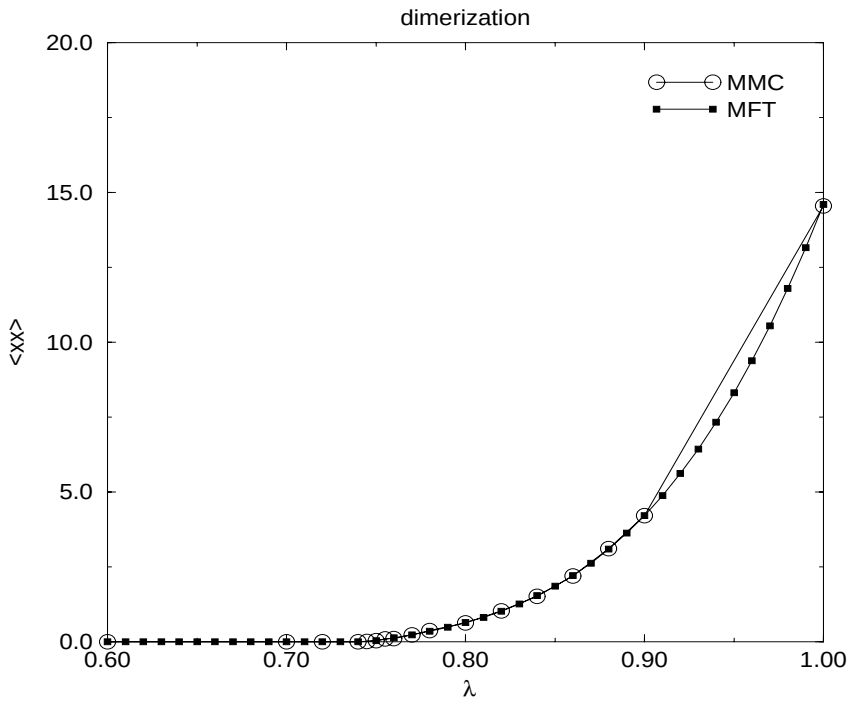

Figure 2-9: *Dimerization correlations* $\langle xx \rangle (k = \pi)$ *for* $T = 0$, $\rho = 1$ *in a 1 dimensional system of 126 sites as a function of the coupling* λ*. The MMC results can be replicated exactly with the Peierls trial state of section 2.4.3.*

For a given phonon state x the electronic system, described by the matrix Q has a spectrum ε_k, and a corresponding density of (single particle) states

$$\Psi'(\varepsilon) = \sum_k \delta(\varepsilon - \varepsilon_k). \tag{2.129}$$

If the phonon state fluctuates this density of states becomes a smooth function

$$\Psi(\varepsilon) = \langle\langle\, \Psi'(\varepsilon)\,\rangle\rangle = \sum_k \langle\langle\, \delta(\varepsilon - \varepsilon_k)\,\rangle\rangle = \int dk \langle\, \varepsilon - \varepsilon(k)\,\rangle. \tag{2.130}$$

In contrast with the previous expectation values, this is a function of a continuous variable that must be averaged. Obviously a delta function is a very poor ingredient for numerical purposes. One could replace it by a histogram counting method: pick a partition of the energy axis and for every realisation of x count the number of eigenvalues in every interval. A more elegant method uses a dynamical correlation function, on which more in chapter 3.

A static operator O is transformed to the time dependent operator $O(t)$ in the Heisenberg picture with

$$O(t) \stackrel{def}{=} e^{-itH} O e^{itH} \tag{2.131}$$

and $O = O(0)$. For creation operators this gives

$$c^\dagger(t) = c^\dagger \cdot e^{itQ(x)}. \tag{2.132}$$

Note that because of the x dependence the right hand side only makes sense within an $\langle\langle \ldots \rangle\rangle$. Now define the Time Dependent Single Particle Density of States as

$$\Psi(t) \stackrel{def}{=} \sum_l \left\langle \left\{\, c_l^\dagger(t)\,,\, c_l \,\right\} \right\rangle \tag{2.133}$$

$$= Sp\, \langle\langle\, e^{itQ}\,\rangle\rangle. \tag{2.134}$$

This can be sampled for a discrete set of t which can then be Fourier transformed to the frequency domain,

$$\Psi(\omega) = \int dt e^{i\omega t} \Psi(t). \tag{2.135}$$

By the properties of the Fourier transform, the width of the intervals in t is related to the maximum frequency (energy) ω sampled and the number of time steps control the resolution in the frequency domain.

Figure 2-10 shows how with the transition to the CDW regime in the half–filled 1–d Holstein model a gap shows up in the Density of States. As explained in section 2.4.3 this transition is a finite–size artifact that arises from the discrete gaps in a finite system. The transition takes place when the dimerization gap equals the finite–size gap.

The fact that the graphs reveal the comb–like structure of individual eigenvalues is due to two circumstances. First, the resolution of the measurement, ie. the number of time steps used to estimate (2.133) was taken large enough, about 4 times the system size L (which is directly proportional to the number of eigenvalues of Q of course. Secondly, for low temperatures the x configuration is frozen to a single state, and the eigenvalues do not wash out over the interval due to thermal fluctuation.

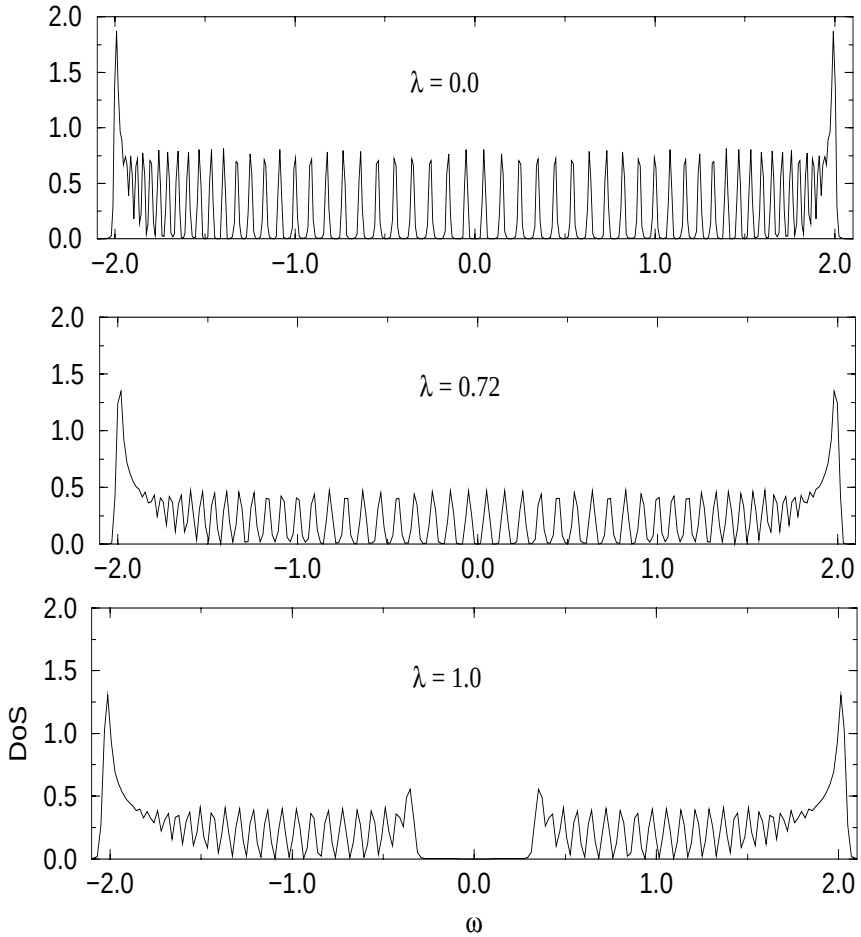

Figure 2-10: *Opening of the gap in the Single Particle Density of states (2.135). MMC Simulation with* $T = 0,\ \rho = 1.0,\ L = 126$, *for* $\lambda = 0.0,\ 0.72,\ 1.0$.

2.5.6 Discussion

The existence of the Peierls state for the 1–dimensional half–filled adiabatic Holstein, Hubbard, SSH and other systems has been strongly suspected, if not proven, since the early work of Fröhlich and Peierls in the fifties. The early numerical work in the eighties by Hirsch, Fradkin and Scalapino dealt with the stability of the Peierls–instability in the Holstein and SSH models against quantum–fluctuations of the lattice, ie. what is called non-adiabaticity in this work[47, 48], and against Coulomb repulsion, ie. a Hubbard term[49]. The latter will not be discussed here.

The results of this section, in particular figure 2-7 reproduce the essence of those authors Quantum Monte Carlo results for heavy ions. Their simulation technique is based on a Trotter decomposition of the partition function that renders it as a sum over world lines of phonons and electrons. The method appears to be stable and practical for temperatures $\beta t < 5$ and lattices up to 40 sites.

They find that only in the anti-adiabatic limit $\hbar\omega \to \infty$ the CDW/dimerisation disappears, however, they notice that in the thermodynamic limit, the critical coupling $\lambda_c = 0$ for any finite ω. Our discussion of the small gap (inversely proportional to L, logarithmically with λ) for finite $L = 4k$ and the finite λ_c for $L = 4k + 2$ answers the question raised in[48] about the small value (numerically indiscernible) of the dimerization at small coupling, and the apparent discrepancy between simulation and analytical result in this range of parameters.

We may conclude that we can perfectly reproduce some important (and undisputed) results from the literature, in an efficient way. The advantage of the present simulation method becomes apparent when considering larger systems, lower temperatures, and most important: the measurement of dynamical correlation functions, the topic of the next chapter. These are not or difficult accessible to other simulation methods (eg. [66]).